Large upper tropospheric ozone enhancements above midlatitude North America during summer: In situ evidence from the IONS and MOZAIC ozone measurement network

O. R. Cooper,[1,2] A. Stohl,[3] M. Trainer,[4] A. M. Thompson,[5] J. C. Witte,[6] S. J. Oltmans,[4]
G. Morris,[7] K. E. Pickering,[8] J. H. Crawford,[9] G. Chen,[9] R. C. Cohen,[10] T. H. Bertram,[10]
P. Wooldridge,[10] A. Perring,[10] W. H. Brune,[5] J. Merrill,[11] J. L. Moody,[12] D. Tarasick,[13]
P. Nédélec,[14] G. Forbes,[15] M. J. Newchurch,[16] F. J. Schmidlin,[17] B. J. Johnson,[4]
S. Turquety,[18] S. L. Baughcum,[19] X. Ren,[5] F. C. Fehsenfeld,[4] J. F. Meagher,[4]
N. Spichtinger,[20] C. C. Brown,[9] S. A. McKeen,[1,2] I. S. McDermid,[21] and T. Leblanc[21]

[1]   The most extensive set of free tropospheric ozone measurements ever compiled across midlatitude North America was measured with daily ozonesondes, commercial aircraft and a lidar at 14 sites during July-August 2004. The model estimated stratospheric ozone was subtracted from all profiles, leaving a tropospheric residual ozone. On average the upper troposphere above midlatitude eastern North America contained 15 ppbv more tropospheric residual ozone than the more polluted layer between the surface and 2 km above sea level. Lowest ozone values in the upper troposphere were found above the two upwind sites in California. The upper troposphere above midlatitude eastern North America contained 16 ppbv more tropospheric residual ozone than the upper troposphere above three upwind sites, with the greatest enhancement above Houston, Texas, at 24 ppbv. Upper tropospheric CO measurements above east Texas show no statistically significant enhancement compared to west coast measurements, arguing against a strong influence from fresh surface anthropogenic emissions to the upper troposphere above Texas where the ozone enhancement is greatest. Vertical mixing of ozone from the boundary layer to the upper troposphere can only account for 2 ppbv of the 16 ppbv ozone enhancement above eastern North America; therefore the remaining 14 ppbv must be the result of in situ ozone production. The transport of NO_x tracers from North American anthropogenic, biogenic, biomass burning, and lightning emissions was simulated for the upper troposphere of North America with a particle dispersion model. Additional box model calculations suggest the 24 ppbv ozone enhancement above Houston can be produced over a 10 day period from oxidation reactions of lightning NO_x and background mixing ratios of CO and CH_4. Overall, we estimate that 69–84% (11–13 ppbv) of the

[1]Cooperative Institute for Research in Environmental Sciences, University of Colorado, Boulder, Colorado, USA.
[2]Also at NOAA Earth System Research Laboratory, Boulder, Colorado, USA.
[3]Norwegian Institute for Air Research, Kjeller, Norway.
[4]NOAA Earth System Research Laboratory, Boulder, Colorado, USA.
[5]Department of Meteorology, Pennsylvania State University, University Park, Pennsylvania, USA.
[6]Science Systems and Applications, Inc., NASA Goddard Space Flight Center, Greenbelt, Maryland, USA.
[7]Department of Physics and Astronomy, Valparaiso University, Valparaiso, Indiana, USA.
[8]Laboratory for Atmospheres, NASA Goddard Space Flight Center, Greenbelt, Maryland, USA.
[9]NASA Langley Research Center, Hampton, Virginia, USA.
[10]Department of Chemistry and Department of Earth and Planetary Science, University of California, Berkeley, California, USA.
[11]Graduate School of Oceanography, University of Rhode Island, Narragansett, Rhode Island, USA.
[12]Department of Environmental Sciences, University of Virginia, Charlottesville, Virginia, USA.
[13]Experimental Studies Research Division, Meteorological Service of Canada, Environment Canada, Downsview, Ontario, Canada.
[14]Laboratoire d'Aerologie, Centre National de la Recherche Scientifique, Observatoire Midi-Pyrenees, Toulouse, France.
[15]Meteorological Service of Canada, Sable Island, Nova Scotia, Canada.
[16]Atmospheric Science Department, University of Alabama, Huntsville, Alabama, USA.
[17]Wallops Flight Facility, NASA Goddard Space Flight Center, Wallops Island, Virginia, USA.
[18]Service d'Aéronomie, Institut Pierre-Simon Laplace, Université Pierre et Marie Curie, Paris, France.
[19]Boeing Company, Seattle, Washington, USA.
[20]Department of Ecology, Technical University of Munich, Freising-Weihenstephan, Germany.
[21]Table Mountain Facility, Jet Propulsion Laboratory, California Institute of Technology, Wrightwood, California, USA.

16 ppbv ozone enhancement above eastern North America is due to in situ ozone production from lightning NO_x with the remainder due to transport of ozone from the surface or in situ ozone production from other sources of NO_x.

1. Introduction

[2] Ozone is a key trace gas for both the chemistry and radiative balance of the troposphere [*Intergovernmental Panel on Climate Change*, 2001], and as it is the principal pollutant associated with photochemical smog its presence in the lower troposphere has large implications for issues of air quality. Currently, international research programs such as the SPARC Project (Stratospheric Processes and their Role in Climate) and IGAC (International Global Atmospheric Chemistry) are focusing research on the dynamics and composition of the upper troposphere and lower stratosphere because of this region's influence on global climate change, with ozone once again a trace gas of primary interest.

[3] Chemical transport model (CTM) studies indicate that North American emissions have a major impact on net global tropospheric ozone production [*Li et al.*, 2002]. However, verifying CTM estimates of the North American ozone budget is difficult because of the limited number of profiling sites across the continent. Long-term ozonesonde profiling has been conducted at six locations in Canada, but all are at relatively high latitudes [*Tarasick et al.*, 2005], and at just two sites in the USA: Boulder, Colorado and Wallops Island, Virginia. However, the National Oceanic and Atmospheric Administration (NOAA) initiated the Trinidad Head, California and Huntsville, Alabama sites in the late 1990s [*Newchurch et al.*, 2003]. Data coverage increased in 2004 with the addition of the NOAA site at Narragansett, Rhode Island, and four new Canadian sites along the USA/Canada border. However, large data gaps still exist in the southwestern and south-central USA and the sampling rate of once per week means it will take several years to build a North American ozone climatology.

[4] To finally measure the daily ozone distribution across midlatitude North America during the most photochemically active part of the year, NASA, NOAA, Environment Canada, and several US universities pooled resources during the 1 July to 15 August 2004 ICARTT (International Consortium for Atmospheric Research on Transport and Transformation) study to launch ozonesondes from several sites across the eastern USA and Canada under the IONS (INTEX Ozonesonde Network Study) program (see overview of IONS by A. M. Thompson et al. (IONS-04 (INTEX Ozonesonde Network Study, 2004): Perspective on summertime UT/LS (upper troposphere/lower stratosphere) ozone over northeastern North America, submitted to *Journal of Geophysical Research*, 2006, hereinafter referred to as Thompson et al., submitted manuscript, 2006)). Additional ozone profiles across eastern North America were obtained from five instrumented commercial aircraft that fly between North America and Europe under the European MOZAIC program. To increase the sample size, MOZAIC profiles were combined with ozonesonde profiles from

nearby locations to form 14 free-tropospheric measurement sites (Figure 1). An additional upper tropospheric ozone monitoring site was available near Los Angeles from combined lidar and MOZAIC measurements. This data set contains the most extensive set of free tropospheric ozone measurements ever compiled across midlatitude North America. In this study we focus on measurements that were made only in the troposphere and subtract the model-estimated stratospheric ozone from each profile leaving a tropospheric residual ozone. An interesting result was that the overall network showed a greater amount of tropospheric residual ozone in the upper troposphere than in the lower troposphere. Furthermore the upper troposphere above eastern North America contained far greater tropospheric residual ozone mixing ratios than the upwind sites, with the largest values above Houston, Texas. We use a particle dispersion model to demonstrate that the upper tropospheric ozone maximum above eastern North America is largely the result of in situ ozone production from lightning NO_x.

2. Method

2.1. Trace Gas Measurements

[5] This study utilizes 260 ozone profiles measured by balloon-borne ozonesondes equipped with electrochemical concentration cell sensors that have an accuracy of about 10% in the troposphere, except when ozone is less than 10 ppbv when accuracies can be degraded to 15% [*Newchurch et al.*, 2003]. Another 183 ozone profiles were measured by five MOZAIC commercial aircraft using a dual-beam UV absorption instrument (Thermo-Electron, model 49–103), with an estimated accuracy of $\pm$ (2 ppbv + 2%) [*Thouret et al.*, 1998]. Sites containing only MOZAIC measurements are New York City, Montreal and Atlanta. Sites containing a combination of MOZAIC and nearby ozonesonde profiles are Houston, Ontario and Washington DC. All other sites contain only ozonesonde measurements. For this study all individual ozone profiles were smoothed in the vertical to 500 m layer averages.

[6] The same five MOZAIC aircraft that measure ozone also measure CO using an infrared carbon monoxide analyzer with a performance suitable for routine aircraft measurements: $\pm$5 ppbv, $\pm$5% precision for a 30 s response time [*Nedelec et al.*, 2003].

[7] The NASA Jet Propulsion Laboratory (JPL) operates two differential absorption ozone lidars at the Table Mountain Facility northeast of Los Angeles to cover the altitude range 4–55 km [*McDermid et al.*, 2002]. The ozone profiles used in this study (5.5 – 27 km) were retrieved using a combination of all the channels of the tropospheric system and one channel of the stratospheric system. For a typical 2-hour integrated nighttime profile the system is accurate to within 5–25% (0.05 to 0.3 $\times$ 10^{12} molecules/cm^3), with
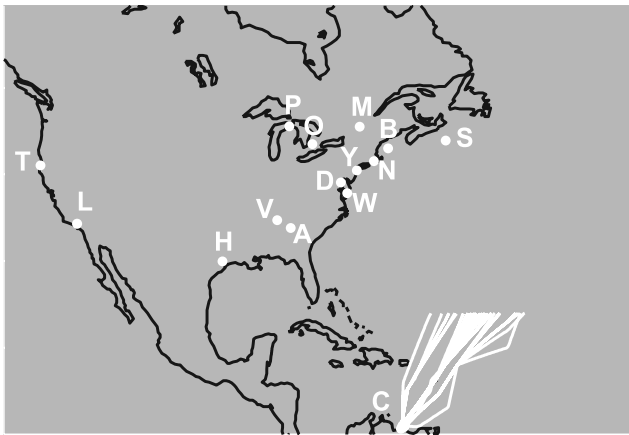
Figure 1. Locations of the fourteen ozone profile sites in 2004: T, Trinidad Head; L, Table Mountain/MOZAIC; H, Houston; V, Huntsville; A, Atlanta; W, Wallops Island; D, Washington DC; Y, New York City; N, Narragansett; B, research vessel *Ronald H. Brown*; S, Sable Island; M, Montreal; O, Ontario; and P, Pellston. The locations of the tropical portions of the MOZAIC flights to and from Caracas (C) during 1999–2004 are also shown.

the largest deviations occurring when the free tropospheric ozone mixing ratios are very low.

[8] Nitrogen Dioxide (NO_2) mixing ratios were measured directly aboard the NASA DC-8 by Laser Induced Fluorescence (LIF) [*Thornton et al.*, 2000; T. H. Bertram et al., Convection and the age of air in the upper troposphere, manuscript in preparation, 2006, hereinafter referred to as Bertram et al., manuscript in preparation, 2006] on all 18 flights during ICARTT above North America and the western North Atlantic Ocean. Briefly, NO_2 is excited at 585 nm using a Nd:YAG pumped tunable dye laser and the resulting red-shifted fluorescence is imaged onto a photomultiplier tube following optical and temporal filtering. A supersonic expansion is used in the detection region to increase the population of NO_2 in the excited rotational state, leading to a factor-of-thirty enhancement in signal [*Cleary et al.*, 2002]. The detection sensitivity of this instrument is 0.8 ppt/min at S/N = 2. The uncertainty in the instrument zero is less than 1 ppt.

[9] NO was measured directly aboard the NASA DC-8 by a commercial NO-NO_x analyzer (Model TEI 42C) on the basis of the chemiluminescence technique. The instrument was run in NO single mode only, and an in situ NO calibration system was used for frequent NO span and background checks. The detection limit of this instrument is about 50 pptv with 1 min integration time.

[10] CO on the NOAA WP-3D research aircraft was measured by vacuum ultraviolet resonance fluorescence with an uncertainty of ±5%. Ozone was measured on the WP-3D with an uncertainty of ±(0.1 ppbv + 3%).

[11] A whole air sampler on board the DC-8 collected air samples in electropolished stainless steel canisters every few minutes during each flight. The canisters were shipped to the University of California, Irvine for analysis. An HP6890 gas chromatogram analyzer with a flame ionization detector was used to measure *i*-pentane and other hydro-

carbons [*Colman et al.*, 2001]. Absolute accuracy was better than 10% at 1σ, with a precision of 3%.

[12] Throughout this manuscript the ozone and CO distributions are compared between sites at 500 m intervals between the surface and the tropopause. We use the Kruskal-Wallace nonparametric one-way analysis of variance test to determine if the trace gas distributions between two given sites have statistically significantly differences at the 95% confidence interval.

2.2. FLEXPART Simulations

[13] The global transport and dispersion of North American NO_x emissions from biomass burning, biogenic, lightning, aircraft and surface anthropogenic sources was simulated with the FLEXPART Lagrangian particle dispersion model [*Stohl et al.*, 1998, 2005], which calculates the trajectories of a multitude of particles. The model was driven by ECMWF wind fields with a temporal resolution of 3 hours (analyses at 0000, 0600, 1200, 1800 UTC; 3 hour forecasts at 0300, 0900, 1500, 2100 UTC), horizontal resolution of $1° \times 1°$, and 60 vertical levels. Nested ECMWF windfields of 0.36° resolution were used for the area between 108°W–18°E and 18–72°N covering the major anthropogenic and lightning emission regions of North America. Both data sets have 16 model layers below 2 km, with 10 layers below 700 m. These data sets approximately represent the full spectral resolution of the ECMWF model at that time. Particles are transported both by the resolved winds and parameterized subgrid motions. To account for convection, FLEXPART uses the parameterization scheme of *Emanuel and Živković-Rothman* [1999], which is implemented at each 15-min model time step, and is intended to describe all types of convection, including the deep convection related to the lightning over the Gulf of Mexico. The scheme was tested by *Forster et al.* [2006] and found to produce convective precipitation amounts that are in relatively good agreement with observations both in the tropics and extratropics, reducing the positive tropical bias of the online convection scheme used at ECMWF. It also improves the agreement of FLEXPART simulations with airborne tracer measurements compared to simulations without the convection parameterization.

[14] FLEXPART is used to simulate the transport of NO_x emissions from biomass burning, biogenic, lightning, aircraft and surface anthropogenic sources. In this study the tracers are run in forward mode as passive tracers that are not removed by wet or dry deposition processes, neither are the NO_x tracers converted to oxidized species. The tracers are tracked for a variety of time periods including 1, 2, 5 10 and 20 days since emission. For example a lightning NO_x tracer that is tracked for 10 days is referred to as a 10-day lightning NO_x tracer. To simulate the oxidation of NO_x in the upper troposphere a 2-day *e*-folding lifetime (as determined from box model analysis) is separately applied to the NO_x tracers from all emission sources.

[15] The stratospheric ozone contribution to each profile was estimated using the FLEXPART retroplume technique [*Stohl et al.*, 2003], as described by *Cooper et al.* [2005a]. Briefly, 40,000 back trajectory particles were released from each 500 m layer of each ozone profile. The number of particles that entered the stratosphere over the previous 20 days was tabulated along with their potential vorticity
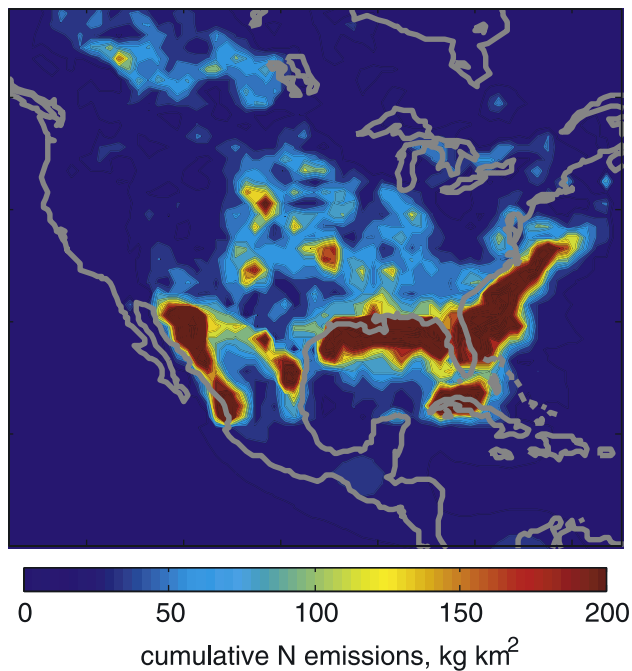
Figure 2. Cumulative lightning N emissions from CG and IC flashes between 21 June and 15 August 2004.

(PV) values. The mass of each particle was scaled by the O_3/PV ratio of the lower stratosphere, as determined from the IONS ozonesondes and ECMWF analyses from the ICARTT study period, to estimate the amount of stratospheric ozone carried by each particle. To account for the fact that the PV value for a given particle changes over time this calculation was performed for each day of the 20-day transport time, with the average calculated ozone value over 20 days considered representative of the particle. This calculation also accounted for the fact that the O_3/PV ratio decreases throughout the summer because of the seasonal decrease of ozone in the lowermost stratosphere. These values were integrated over all 40,000 particles in a given retroplume to yield the quantity of stratospheric ozone influencing a particular 500 m layer of an ozone profile. To verify the modeled results, the ratio of modeled/measured ozone values was calculated for all IONS ozonesonde profiles for each 500 m layer in the stratosphere (PV >2). The geometric mean of all the point-by-point ratios of modeled/measured ozone was near unity (0.97), indicating little overall bias in the model. The standard error of the modeled stratospheric ozone compared to measured ozone was a factor of 1.5.

2.3. Lightning NO$_x$ Emissions

[16] The lightning NO$_x$ emissions in this study are not produced by a grid-scale model parameterization scheme. Instead, lightning NO$_x$ production was simulated with FLEXPART above North America and the surrounding waters according to the exact times and locations of each cloud-to-ground (CG) lightning flash observed by lightning detection networks. To the best of our knowledge this is the most accurate simulation of lightning NO$_x$ emissions ever conducted for all of North America. CG flashes were detected over the continental USA by the National Lightning

Detection Network (NLDN), with a detection efficiency (DE) better than 90% [*Grogan*, 2004]. For regions between 21 and 60°N, but outside of the continental USA, CG flashes were detected with the experimental long-range lightning detection network (LRLDN). DE is 60–80% at 60°N and 40–60% at 21°N and increases with proximity to the USA (K. Cummins, Vaisala-Thunderstorm, personal communication, 2005). For regions south of 21°N CG and IC flashes were quantified according to a seasonally and diurnally varying climatology based on 5 years of data from the polar orbiting Lightning Imaging Sensor (LIS) and Optical Transient Detector (OTD) instruments [*Christian et al.*, 2003].

[17] To account for the drop-off in detection efficiency south of the USA all NO$_x$ emissions from LRLDN flashes in this region were scaled by the inverse of the DE. Furthermore we scaled the NO$_x$ emissions per CG flash to account for the intracloud (IC) flashes not detected by the NLDN and LRLDN [*Ridley et al.*, 2005]. Monthly gridded IC:CG ratios calculated for the continental United States were applied to the NLDN data [*Boccippio et al.*, 2001]. Monthly mean IC:CG values typically range between 1 and 10 for individual 0.5° × 0.5° grid cells, with an average value of 4.2 above the continental USA during the study period of 21 June through 15 August. This average value of 4.2 was applied to the LRLDN data.

[18] We selected a lightning NO$_x$ emission rate of 6.4 kg N flash^{-1} on the basis of the analysis of North American thunderstorms by *DeCaria et al.* [2005]. Between 21 June and 15 August 2004, a single FLEXPART trajectory particle was released at the exact time and location of the 32 million CG lightning flashes detected by the NLDN and LRLDN. Another 15 million trajectory particles were released from the region of the lightning climatology (representing 30 million IC and CG flashes). Computer memory limitations only permitted the release of one FLEXPART particle per flash. To account for the fact that lightning NO$_x$ emissions occur mainly in the upper troposphere but over a wide range of altitudes [*Pickering et al.*, 1998; *DeCaria et al.*, 2005], the particles were released between the tropopause and 6 km above sea level according to a normal distribution which was allowed to slide up and down with the height of the tropopause. No particles were released below 6 km and the mode of the release height was between 10 and 11 km. Upon release the particles were permitted to move vertically according to the model vertical winds and the convection scheme.

[19] The distribution of the lightning N emissions is shown in Figure 2. The major regions for lightning emissions are located (1) along the Sierra Madre Mountains of northwestern Mexico, (2) above Cuba, and (3) a band stretching along the northern coast of the Gulf of Mexico, extending across Florida and into the westernmost North Atlantic Ocean off the southeastern USA. Lightning is also prevalent across the USA, east of the Rocky Mountains. These lightning regions generally correspond to the most intense regions of lightning depicted by lightning climatologies [*Christian et al.*, 2003; *Orville et al.*, 2002]. The exception is that the lightning along the northern coast of the Gulf of Mexico extends further south than shown by *Christian et al.* [2003], and the lightning is relatively more intense off the coast of the southeastern USA than shown by

Christian et al. [2003]. These lightning regions correspond to precipitation maxima above the northern Gulf coast and the westernmost North Atlantic Ocean during summer 2004 (as shown in monthly precipitation plots produced by the Global Precipitation Climatology Project (GPCP)) and are the result of several cold fronts that pushed offshore during the study period. The lightning emissions south of 21°N are tied to the lightning climatology of *Christian et al.* [2003] and appear very diffuse in comparison to the NLDN and LRLDN lightning emissions because of heavy smoothing over $2.5° \times 2.5°$ grid cells and boxcar smoothing across several weeks.

[20] Multiplying our lightning NO_x emission rate by the global lightning flash rate of 44 flashes s^{-1} as determined from satellite observations [*Christian et al.*, 2003] yields a global lightning NO_x production of 8.9 Tg N year^{-1}. The 47 million FLEXPART particles in the simulation represent the transport of 1.2 Tg of lightning N from 194 million IC and CG flashes over the study region between 21 June and 15 August 2004. These emissions occur during the peak lightning season in one of the world's most intense lightning regions, especially in southeastern North America [*Zipser et al.*, 2006], and represent an estimated 13% of the assumed 8.9 Tg global annual lightning N emissions.

2.4. Other NO_x Emission Inventories

[21] North American emissions were based on the point, on-road, nonroad and area sources from the U.S. EPA National Emissions Inventory, base year 1999, with spatial partitioning of area type sources at 4 km resolution. This database covers the USA, Mexican emissions north of 24°N, and all Canadian sources south of 52°N [*Frost et al.*, 2006]. Emissions for all other regions of North America and the rest of the Northern Hemisphere were taken from the EDGAR 3.2 Fast Track 2000 data set, which estimates year 2000 emissions using the EDGAR 3.2 estimates for 1995 and trend analyses for the individual countries. EDGAR uncertainty estimates are roughly 50% or greater [*Olivier and Berdowski*, 2001].

[22] Biomass burning NO_x tracer was released from a $1° \times 1°$ grid of daily average emissions from forest and peat fires (S. Turquety et al., Inventory of boreal fire emissions for North America: Importance of peat burning and pyroconvective injection, submitted to *Journal of Geophysical Research*, 2006). The emission inventory for North America was generated using MODIS hot spots and reported area burned and information on type of vegetation, fuel loading, and emission factors. Emissions for the rest of the world are based on 2004 monthly MODIS hot spots. The biomass burning NO_x tracer was emitted between the surface and 5000 m as an attempt to account for the uncertain altitude reached by the hot and buoyant boreal smoke plumes.

[23] An aircraft NO_x tracer was released in the Northern Hemisphere using a global emission inventory of aircraft emissions created by combining the civil traffic inventory for 1999 of *Sutkus et al.* [2001] with an estimate for 1999 military, charter, and general aviation obtained by extrapolating the earlier inventory work of *Mortlock and Van Alstyne* [1998]. Emissions in these inventories were calculated using great circle routes and provided on a $1° \times 1°$ by 1 km altitude grid for each month of 1999. Actual civil aircraft routes vary from day to day because of air traffic

congestion, prevailing winds or to avoid turbulence. The use of idealized great circle routes as opposed to actual flight routes can result in some errors but this has been found to be relatively small ($\sim$5%) [*Forster et al.*, 2003].

[24] Soil biogenic NO_x emissions are prescribed according to the Biogenic Emissions Inventory System version 3.11 (BEISv3.11) available through the U.S. EPA (ftp://ftp.epa.gov/amd/asmd/beis3v11). These emissions are based on the vegetative-dependent emission parameters within BEIS2 (normalized at 30°C) and the 1 km horizontal resolution Biogenic Emissions Landuse Database (BELD) as outlined in *Pierce et al.* [1998]. BEIS3 updates to soil NO_x emissions include canopy recapture factors, and day-of-year specific correction factors for growing season and fertilization rates given by *Yienger and Levy* [1995].

[25] An auxiliary animation[1] of the FLEXPART lightning NO_x tracer is included with this paper. While the animation is not essential for understanding the results presented here, viewing it allows the reader to clearly see the temporal and spatial evolution of the lightning NO_x tracer. The animation shows the location of a 10-day lightning NO_x tracer expressed as a column value above North America and the North Atlantic Ocean, every two hours between 1 July and 15 August 2004.

3. Results

3.1. A Case Study of Unexpectedly Large Ozone Mixing Ratios in the Upper Troposphere

[26] On the afternoon of 27 July 2004 the NOAA WP-3D instrumented aircraft flew a survey mission of the lower troposphere from New Hampshire to Virginia to investigate air pollution in the warm sector of a midlatitude cyclone that was traversing the eastern USA. The warm sector is the component of a midlatitude cyclone located ahead of the surface cold front and typically associated with the buildup and large-scale export of emissions along the eastern seaboard of North America [*Merrill and Moody*, 1996; *Moody et al.*, 1996]. Geostationary satellite images of the cyclone showed the three typical airstreams of a midlatitude cyclone: the clear, dry airstream behind the cold front, the cloudy cold conveyor belt north of the warm front, and the cloudy warm conveyor belt (WCB) which flows through the warm sector [*Cooper et al.*, 2002]. However, closer inspection of the WCB showed that the cloud shield was not formed in the typical manner of quasi-isentropic ascent ahead of and parallel to the cold front, as observed in autumn, spring and winter. Instead, in this summertime cyclone the upper level clouds were almost entirely the result of convective outflow from the widespread thunderstorms that occurred within the warm sector above the southeastern USA from 25 to 28 July.

[27] The extensive thunderstorm activity during this 4-day period is illustrated by more than 500,000 cloud-to-ground lightning flashes detected by the NLDN in Figure 3a. The NOAA WP-3D spent several hours dodging thunderstorms as it sampled the lower troposphere. The convection became so severe over Pennsylvania that this sturdy aircraft that routinely conducts research flights through the eye-

---

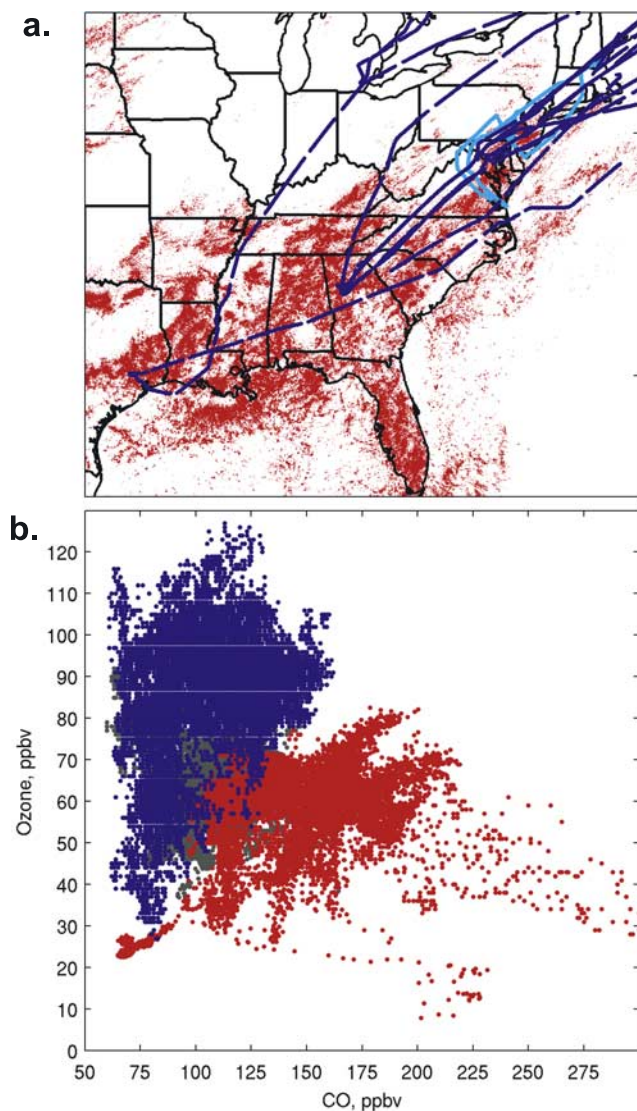[1]Auxiliary materials are available in the HTML. doi:10.1029/2006JD007306.

Figure 3. (a) All MOZAIC flight segments (dark blue) that passed through the warm sector of the midlatitude cyclone that traversed the eastern USA from 25 July through 28 July 2004. Also shown are the flight track of the NOAA WP-3D on 27 July (light blue) and all cloud-to-ground lightning flashes during 25–28 July (red). (b) All ozone versus CO measurements from the NOAA P3 and MOZAIC aircraft within the troposphere of the cyclone warm sector during 25–28 July: 0.0–2.0 km (red), 2.0–8.0 km (gray), and 8.0–12.0 km (blue).

walls of hurricanes aborted the mission and returned to its base in New Hampshire by flying far ahead of the storms via the calmer air above the ocean. The lightning NO_x generated by the thunderstorms during this time period was advected toward the northeast along the east coast, steered by the winds within the warm sector and illustrated in the supplemental lightning NO_x animation.

[28] During the 25–28 July time period in which the cyclone influenced air mass transport along the east coast 17 MOZAIC flights passed through the warm sector within the troposphere. All of the ozone and CO measurements from the cruising altitude and ascent/descent portions of these flights, along with the 27 July WP-3D flight are shown in Figure 3b. These data represent the most extensive set of ozone and CO measurements ever reported for a single cyclone warm sector above the USA. Figure 3b shows that the polluted lower troposphere is associated with ozone up to 83 ppbv. In contrast the less polluted upper troposphere has many data points with ozone greater than 83 ppbv, reaching a maximum of 127 ppbv. Because of the extensive convection within the warm sector the upper troposphere is heavily influenced by air parcels transported from the surface of the eastern USA, but the dilution associated with convection resulted in CO mixing ratios below 162 ppbv. The upper tropospheric ozone mixing ratios above 83 ppbv are associated with CO mixing ratios that range from 61 to 162 ppbv, with no correlation. The fact that east coast polluted air masses lofted to the upper troposphere experience dilution of CO but a strong increase in ozone indicates that these air parcels are either being mixed with an upper tropospheric reservoir of high ozone/low CO air, and/or the air masses are experiencing free tropospheric ozone production. We do not believe that stratospheric air is playing a large role in the upper tropospheric ozone enhancement because all measurements were made far ahead of the stratospheric ozone typically found in the cyclone's dry airstream that descends west of the cold front and the warm sector [*Cooper et al.*, 2002]. The warm sector air had a strong subtropical origin and our FLEXPART stratospheric ozone simulation indicates no more than 14% of the upper tropospheric ozone can be attributed to an aged stratospheric origin. We conclude that the ozone enhancement in the upper troposphere must have been produced in situ and we demonstrate in the rest of this manuscript that the dominant source is most likely ozone production involving lightning generated NO_x.

3.2. Tropospheric Ozone Distribution Across Midlatitude North America

[29] Figure 4a shows the median and standard deviation ozone profiles at the 13 sites that provide full tropospheric and stratospheric measurements during the ICARTT study period. Ozone is much greater in the 6–12 km range than in the lower troposphere and the standard deviation is also generally greater at these altitudes, but much of this influence is due to a stratospheric ozone component. The influence from the stratosphere results from a lower tropopause when a site is north of the polar jet stream and from stratospheric intrusions which are common at midlatitudes, even in summer [*Moody et al.*, 1996; Thompson et al., submitted manuscript, 2006]. The only site with a low standard deviation in the upper troposphere is Houston which is located south of the summertime range of the polar jet stream.

[30] The aim of this study is to focus on purely tropospheric measurements requiring the removal of any recent stratospheric influence. We first removed any part of any individual profile with a PV value greater than 1.0 pvu, which removed the stratospheric influence associated with a low tropopause or fresh stratospheric intrusions (typically less than 2–3 days old). At this point any 500 m layer at any site with less than 10 remaining profiles was dropped from the analysis. The median tropospheric ozone profiles are shown in Figure 4b. Above 4 km the ozone values and
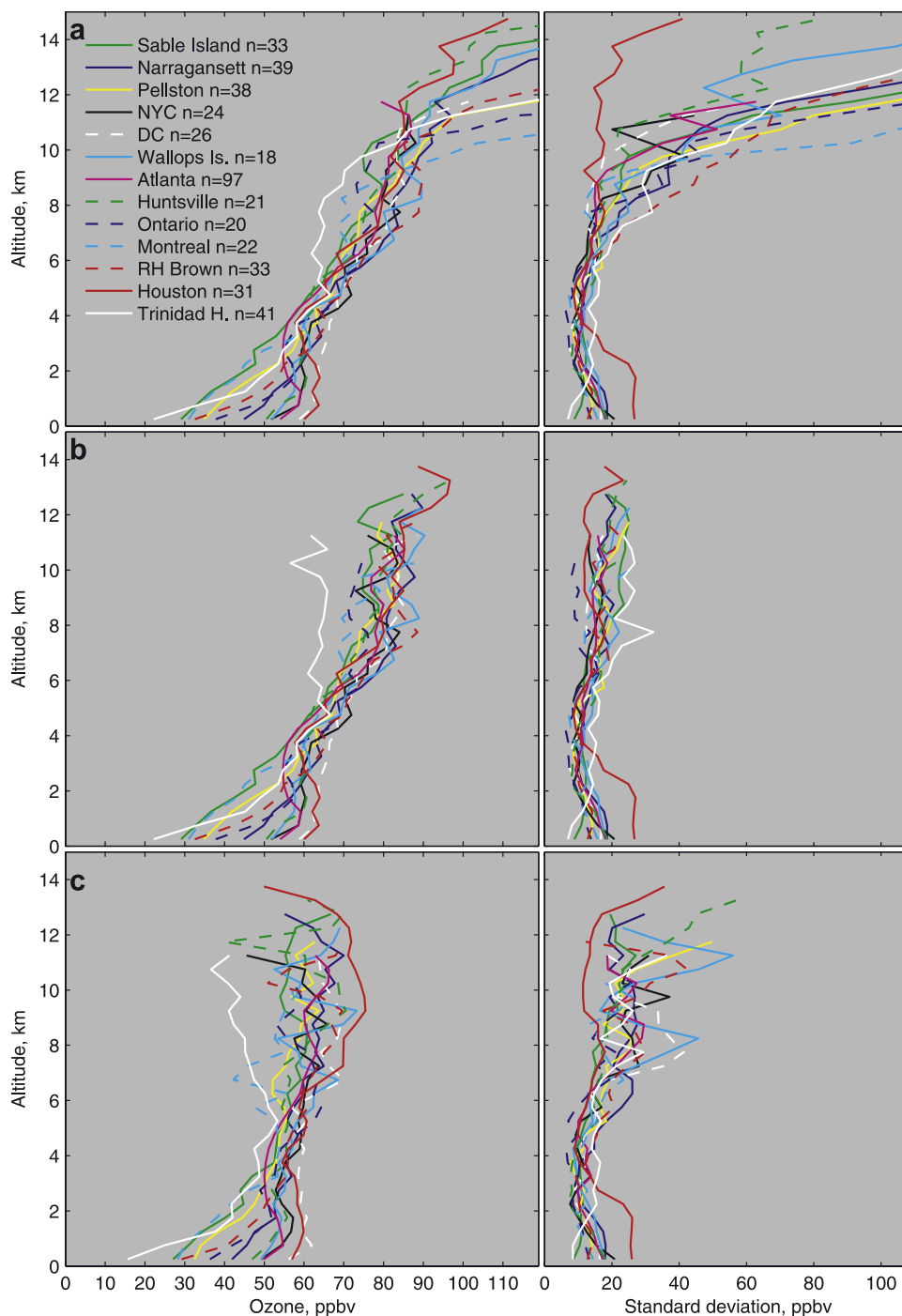
Figure 4. (a) Median ozone profiles at all thirteen sites for 1 July to 15 August 2004, reported in 500 m layers with the sample size indicated by n, and the corresponding standard deviations to the right. (b) Median ozone profiles for measurements taken only within the troposphere (PV < 1.0) and the corresponding standard deviations to the right. (c) Median ozone profiles after the estimated stratospheric influence from the past 20 days has been removed, with standard deviations to the right.

standard deviations decrease at all 13 sites compared to the profiles in Figure 4a.

[31] We then subtracted from each individual profile the contribution from the stratosphere as determined by the FLEXPART retroplume technique, removing any influence from aged stratospheric intrusions up to 20 days old. The proportion of stratospheric ozone in the upper troposphere (greater than 8 km altitude and PV < 1.0) ranged from an average of 27% at Trinidad Head on the west coast to 13% at Sable Island on the east coast. Trinidad Head was immediately downwind of a region of highly active stratosphere-to-troposphere transport. In contrast Sable Island was not strongly influenced by stratospheric intrusions during summer 2004 because of predominantly southerly transport from the tropical and subtropical North Atlantic troposphere.

[32] Once the stratospheric influence from the previous 20 days has been removed, the ozone profiles are referred to as tropospheric residual profiles (a quantity which should not be confused with the tropospheric ozone residual that can be calculated from Total Ozone Mapping Spectrometer data [*Fishman et al.*, 1990; *Fishman and Balok*, 1999]). The median and standard deviation tropospheric residual profiles for each site are shown in Figure 4c. The standard deviations of the tropospheric residual ozone profiles in the upper troposphere are greater than the tropospheric profiles in Figure 4b because of errors in the calculation of the stratospheric ozone component; Wallops Island stands out as being particularly noisy because of its small sample size (n = 18). *Cooper et al.* [2005b] demonstrated that FLEXPART simulates well the transport and decay of stratospheric intrusions far south of their origin along the polar jet stream, capturing the transport of intrusions from the midlatitude lower stratosphere to the lower troposphere and the marine boundary layer of the tropical Pacific Ocean. In that study FLEXPART performed with little bias but with a standard error of 1.5. Much of this error was due to timing differences between the simulated intrusions and measurements (as much as 12–15 hours), or relatively small displacements of modeled intrusions in the vertical. The rest of the error was due to errors in the wind fields and ozone variability in the lower stratosphere not captured by the average ozone/PV relationship. In the present study FLEXPART also has a standard error of 1.5 so the modeled and measured ozone values for a given time and location will differ by an average factor of 1.5. However, because the model has been shown to perform with little bias and can resolve decaying intrusions, the average influence of stratospheric intrusions at a given location is expected to be fairly accurate.

[33] The tropospheric residual ozone profiles represent the median amount of ozone in the troposphere at a given site with either a tropospheric origin or an aged stratospheric origin greater than 20 days. We assume that any remaining stratospheric ozone older than 20 days is dispersed throughout the midlatitude troposphere and we neglect any weak latitudinal gradient that may still exist. Below 5 km the tropospheric residual ozone profiles are representative of transport along all of the typical pathways that influence a site. Above 5 km where portions of profiles have been removed because of the presence of a low tropopause or strong stratospheric intrusions the profiles are biased away from air masses with polar origins. This bias increases with altitude with profiles above 10 km representative of air masses with midlatitude or tropical origins, as expected for tropospheric air masses at these altitudes.

[34] An interesting result is that the tropospheric residual ozone profiles show an overall increase of ozone with altitude even though the greatest concentrations of anthropogenic ozone precursors are found near the surface (Figure 4c). When stations are considered individually all have significantly more ozone in the upper troposphere (>6 km) than in the lower troposphere (<2 km). When data from all sites are combined the difference is also statistically significant with a median tropospheric residual ozone value of 61 ppbv in the upper troposphere and 46 ppbv in the lower troposphere. When considering just the 12 eastern North America sites the median tropospheric residual ozone value in the upper troposphere is 62 ppbv, and 47 ppbv in the lower troposphere.

[35] The lone western North America site of Trinidad Head has, by far, the lowest tropospheric residual ozone values in the upper troposphere. In comparison, the 12 sites in eastern North America show a broad upper tropospheric ozone enhancement. Houston has the greatest values, otherwise none of remaining eleven eastern sites clearly dominates. In comparison to these combined eleven eastern sites, Houston has significantly more ozone between 7.5 and 11.0 km.

3.3. Determining Upper Tropospheric Ozone Values Upwind of North America

[36] Because of the predominantly westerly transport across midlatitude North America it is convenient to treat Trinidad Head as an ozone monitoring site with upper tropospheric ozone values typical of the air masses that enter western North America from the North Pacific Ocean and subsequently travel across the continent. Figure 5 shows the difference in median tropospheric residual ozone values between each site in eastern North America and the upwind site of Trinidad Head, and also indicates when the differences are statistically significant. North of 44°N Montreal shows no statistically significant difference in ozone above 6 km, but Sable Island and Pellston have several layers with significantly more ozone. In the northeastern USA, the sites of New York City (NYC), Narragansett and the research vessel *Ronald H. Brown* in the Gulf of Maine have 20–30 ppbv excess ozone at 8–11 km, while Ontario further west shows mainly insignificant enhancements. In general the upper tropospheric ozone enhancements are even greater in the southeastern and southern USA with Houston showing the overall greatest enhancements. Enhancements in the southern USA below 1 km are even greater than the upper tropospheric enhancements, but are not so remarkable as strong summertime ozone production near the surface of the southern USA is well documented [*Fiore et al.*, 1998]. Furthermore, these values are compared to very low ozone mixing ratios at Trinidad Head that are mainly representative of the marine boundary layer and lower troposphere of the Pacific Ocean.

[37] This comparison indicates a broad upper tropospheric ozone maximum above eastern North America which increases in magnitude toward the south until it reaches a maximum above Houston. However, is Trinidad Head truly representative of the ozone flowing into North America, and is it truly upwind of the eastern North America sites? To explore this question we provide ozone measurements from two additional sites: Table Mountain/MOZAIC and Caracas/eastern Caribbean.

[38] The Table Mountain/MOZAIC ozone monitoring site contains a combination of ozone profiles from the JPL Table Mountain tropospheric lidar located 60 km northeast of downtown Los Angeles and a MOZAIC aircraft. During the ICARTT study period the lidar produced 17 profiles above 4 km altitude. In the same period a MOZAIC aircraft made 22 flights to and from Los Angeles International Airport, but because of instrument problems only 9 ozone profiles were available in the upper troposphere. These 9 profiles were combined with the 17 lidar profiles and the tropospheric residual ozone was calculated for each 500 m layer.
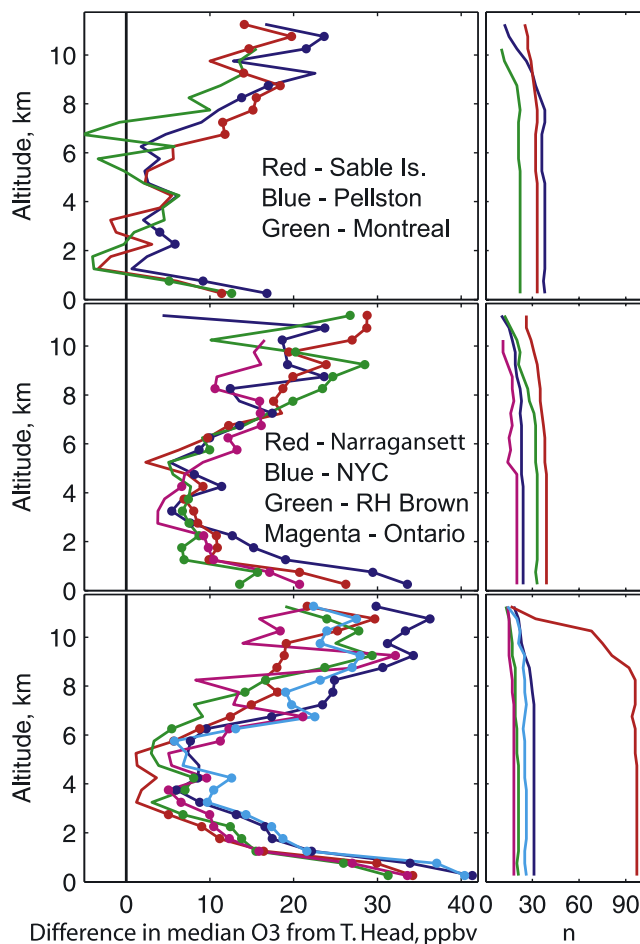
Figure 5. Difference in median O_3 values between sites in eastern North America and Trinidad Head. Solid circles on the profiles indicate the 500 m layers with O_3 distributions that are significantly different from Trinidad Head at the 95% confidence interval. The sites are partitioned into three regions: (top) north of 44°N, (middle) northeast USA or eastern Canada, and (bottom) Mid-Atlantic or southern states. Shown are Houston (blue), Atlanta (red), Huntsville (green), Wallops Island (magenta), and Washington DC (cyan). The right hand plots indicate the sample size in each 500 m layer.

[39] We searched the MOZAIC database for ozone profiles south of the USA to determine the ozone mixing ratios that flow into the southern USA with the North American Monsoon which dominates the transport patterns of the southern USA during July and August. We could only find six profiles south of the USA during the ICARTT study period, however we did find 91 flights to and from Caracas, Venezuela during July August from 1999 to 2004, which we used to construct a multiyear composite ozone profile. The flight tracks of the tropical portions of these flights are shown in Figure 1. Comparison of these flight tracks to the column lightning NO_x emissions in Figure 2 shows that they pass through the tropical easterlies upwind of the regions strongly influenced by North American lightning. They are also upwind of the North American monsoon flow,

and therefore provide some information on the background ozone entering the southern USA.

[40] Figure 6a shows the average circulation at 250 hPa above North America during July and August 2004. An upper level trough was located over eastern North America, while an upper level ridge was located above central North America with a closed anticyclonic circulation above the northern coast of the Gulf of Mexico. This upper level anticyclone maintained the monsoon flow above North America during the study period and is the same feature described by *Li et al.* [2005] that is important for trapping convective outflow above southern North America during summer. Figure 6 also shows the average location of eleven million trajectory particles released continuously during the study period between the tropopause and 6 km altitude above each upwind site. Air masses from the upper troposphere above Trinidad Head follow the ridge/trough pattern in Figure 6a and pass directly through the upper troposphere of the ozone measurement sites in the eastern USA and Canada, with lesser influence above the sites in the southern USA. However, the air masses above Table Mountain/Los Angeles have a stronger influence on the upper troposphere above the southern USA. In contrast, the air masses from the eastern Caribbean have more variable transport pathways but in general have a strong influence across the southern Caribbean with weak and diffuse transport into the southern USA. While this location is not a persistent upwind source region for the southern USA it still provides useful information on background upper tropospheric ozone in a region well known for its association with the summertime transport of tropical storms, hurricanes and Saharan dust storms from the tropical North Atlantic Ocean into the Caribbean and southern USA.

[41] Figure 7 compares the median tropospheric residual ozone profiles above Houston to Trinidad Head, Caracas and Table Mountain/MOZAIC. All 500 m layers above 6 km contain significantly more ozone above Houston than above these three upwind sites. For good measure we also include the median ozone profile above Hilo, Hawaii in Figure 7d which is at the upwind end of a transport pathway from Hawaii to Houston, indicating that the upper troposphere of the remote North Pacific Ocean has even less ozone than the three upwind sites on the edge of North America.

[42] Median tropospheric residual ozone values above 6 km at Trinidad Head, Table Mountain/MOZAIC and Caracas are 45 ppbv, 45 ppbv and 49 ppbv respectively. Taking the average of these three sites we estimate that the overall upwind tropospheric residual ozone mixing ratio above 6 km is 46 ppbv. The corresponding value above all 12 sites in eastern North America is 62 ppbv, ranging from 54 ppbv above Montreal to 70 ppbv above Houston. Because we have already removed the stratospheric influence the ozone enhancement of roughly 16 pbbv in the upper troposphere above eastern North America can only come from two sources: transport of ozone from the lower troposphere to the upper troposphere or in situ ozone production in the free troposphere. Estimating the influence of lower tropospheric ozone on the upper troposphere is difficult because of its temporal and spatial variability across North America. However, let us assume the ozone values from the 12 eastern North America sites, that were predominantly measured in
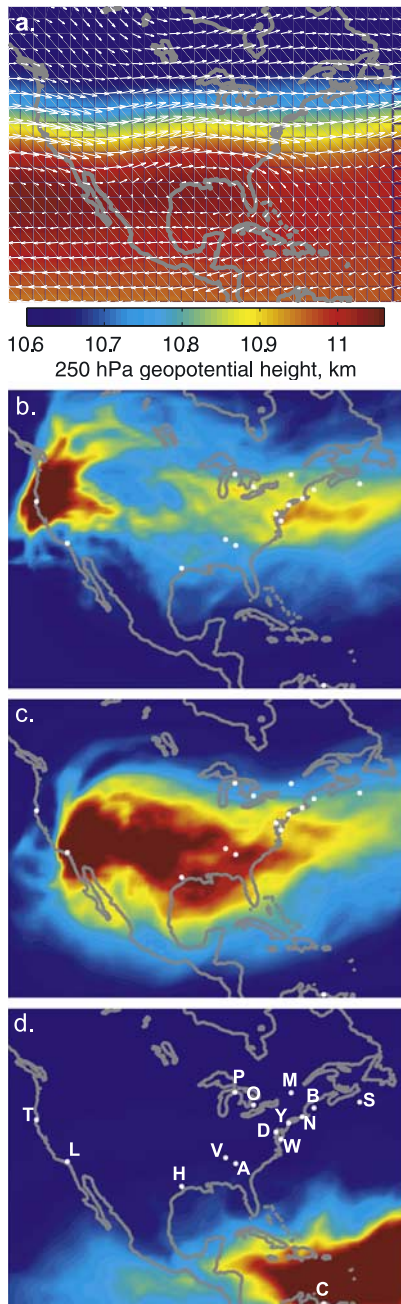
Figure 6. (a) Average July and August 2004 250 hPa geopotential height and wind vectors. Eleven million trajectory particles were released between 6 km above sea level and the tropopause during the study period from (b) Trinidad Head, (c) Los Angeles and (d) the eastern edge of the Caribbean and were allowed to advect for 20 days. Shown are the average locations of the trajectories (in arbitrary units) above 6 km. The locations of the ozone profile stations are indicated: T, Trinidad Head; L, Table Mountain/Los Angeles; H, Houston; V, Huntsville; A, Atlanta; W, Wallops Island; D, Washington DC; Y, New York City; N, Narragansett; B, research vessel *Ronald H. Brown*; S, Sable Island; M, Montreal; O, Ontario; P, Pellston; and C, Caracas.
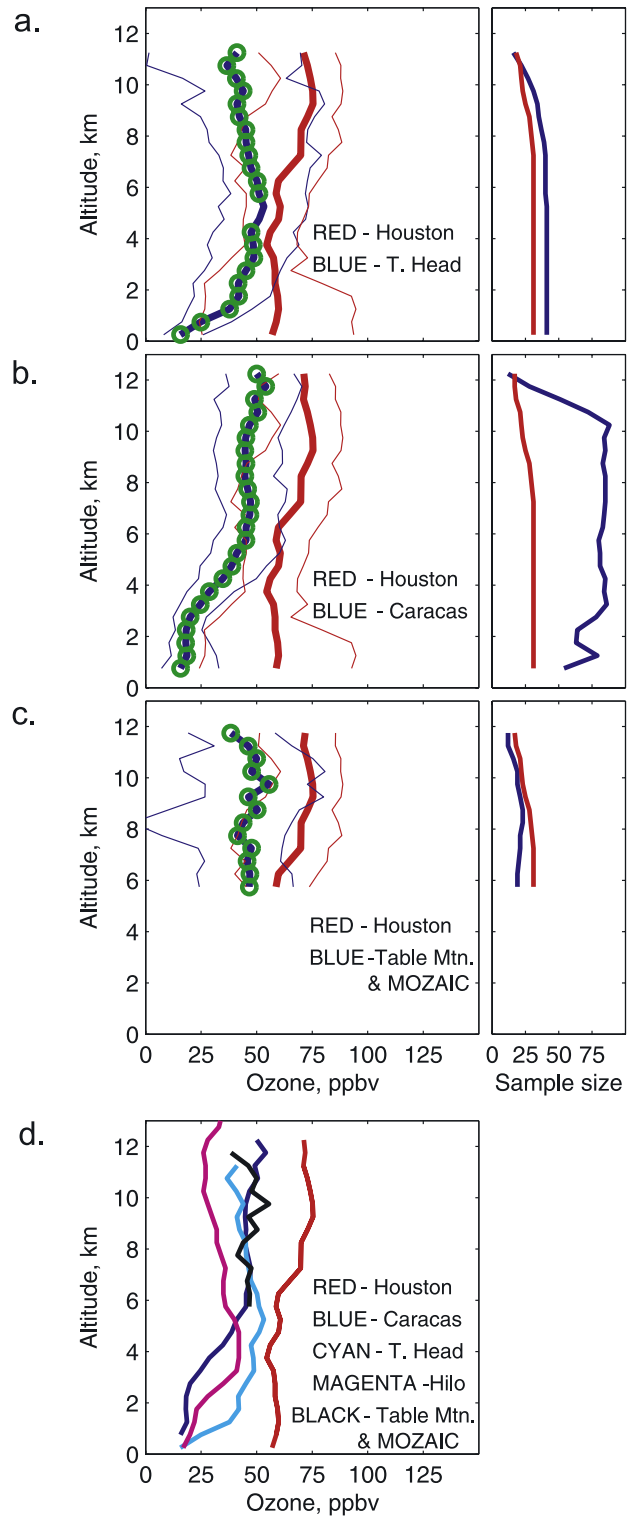

Figure 7. Comparison of ozone distributions between (a) Houston and Trinidad Head, (b) Houston and Caracas, and (c) Houston and Table Mountain/MOZAIC. Shown are median values (thick lines) and 10th and 90th percentiles (thin lines), with green circles indicating those 500 m layers with ozone distributions that are significantly different at the 95% confidence interval. (d) Comparison of median ozone values at Houston to the upwind sites of Caracas; Trinidad Head; Table Mountain/MOZAIC; and Hilo, Hawaii, which has 62 profiles in July and August from 1999 to 2005.
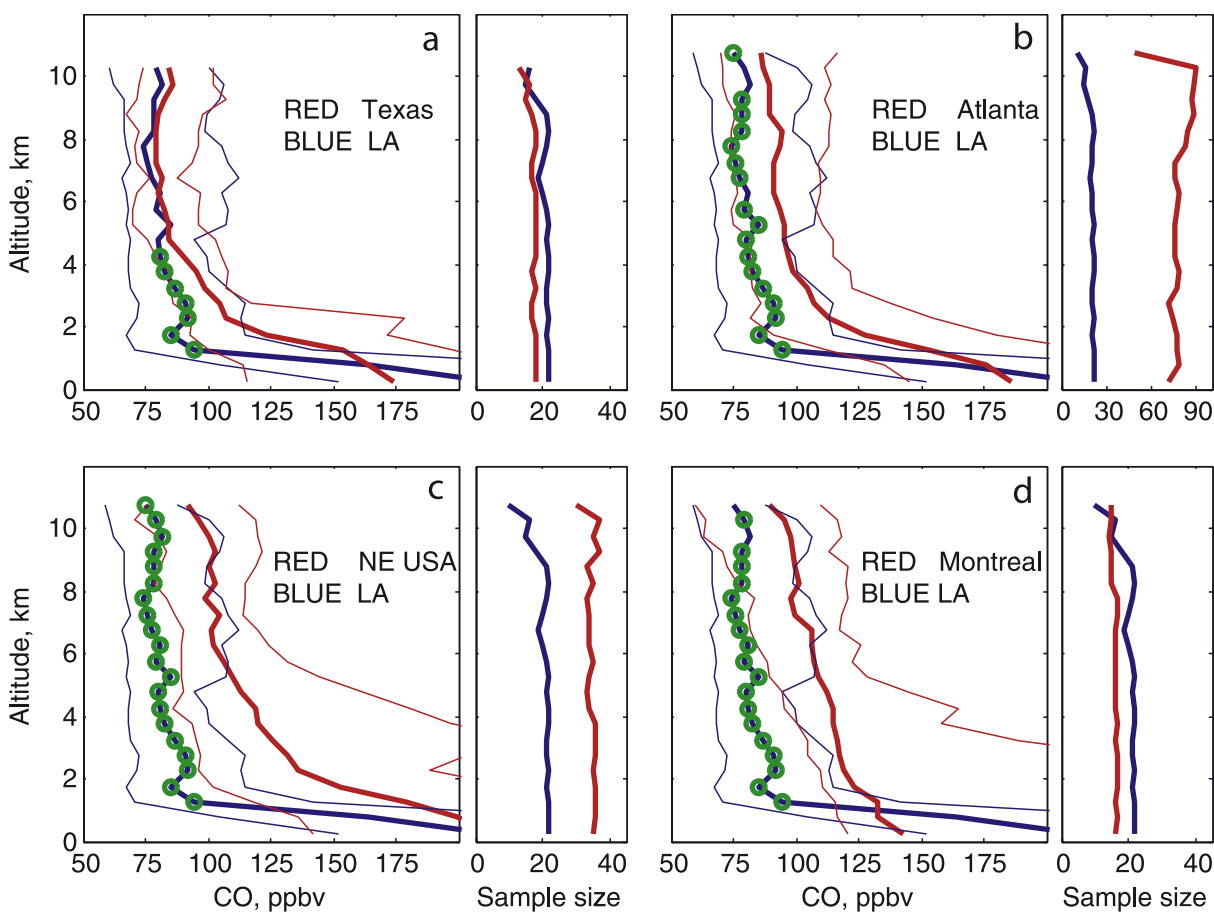
Figure 8. MOZAIC CO distribution above (a) Texas (Houston and Dallas), (b) Atlanta, (c) northeastern USA (New York City and Boston), and (d) Montreal, compared to the median values above Los Angeles during 1 July to 15 August 2004. Shown are median values (thick lines) and the 10th and 90th percentiles (thin lines), with green circles indicating those 500 m layers at the downwind sites that have a CO distribution statistically significant from Los Angeles at the 95% confidence interval. Sample sizes are indicated to the right of each plot.

early afternoon or early evening, are broadly representative of North American lower tropospheric ozone during the ICARTT study period. The average tropospheric residual ozone value of the eastern North America lower troposphere (< 2 km) is 47 ppbv, only one ppbv greater than the upper tropospheric value of the upwind sites. So no matter how much air is transported from the surface of eastern North America and mixed with the air from the upwind sites as it enters the upper troposphere above eastern North America, on average, the upper tropospheric ozone value cannot rise above 47 ppbv because of mixing alone. Even if we are very cautious and assume the median ozone mixing ratio of 59 ppbv in the lower troposphere above Houston is representative of eastern North America and assume all of the eastern North America upper troposphere is exposed to the same amount of vertical mixing as Houston (FLEX-PART indicates 15% of the mass of the upper troposphere above Houston originates in the mixed layer over the previous 20 days) upper tropospheric ozone would never exceed 48 ppbv because of mixing alone. Therefore at least 14 ppbv of the 16 ppbv ozone enhancement above eastern

North America must be the result of in situ ozone production in the free troposphere.

3.4. Relatively Low Pollution Levels in Upper Troposphere Above Houston

[43] Now that we have established that in situ ozone production is responsible for the majority of the upper tropospheric ozone enhancement above eastern North America we must determine the relative impact of NO_x emissions from lightning, biomass burning, biogenic, aircraft and surface anthropogenic sources. However, first we will focus on the upper troposphere of Houston to illustrate that this region is not heavily influenced by pollution and that the ozone production above this site must be strongly associated with lightning NO_x.

[44] In situ evidence that the upper troposphere above Houston and east Texas is not heavily polluted comes from the CO profiles measured by MOZAIC aircraft during the ICARTT study period. Figure 8a compares the CO distributions above Los Angeles to the CO distribution above east Texas (flights to and from Houston and Dallas). Above 5 km there is no statistically significant difference between
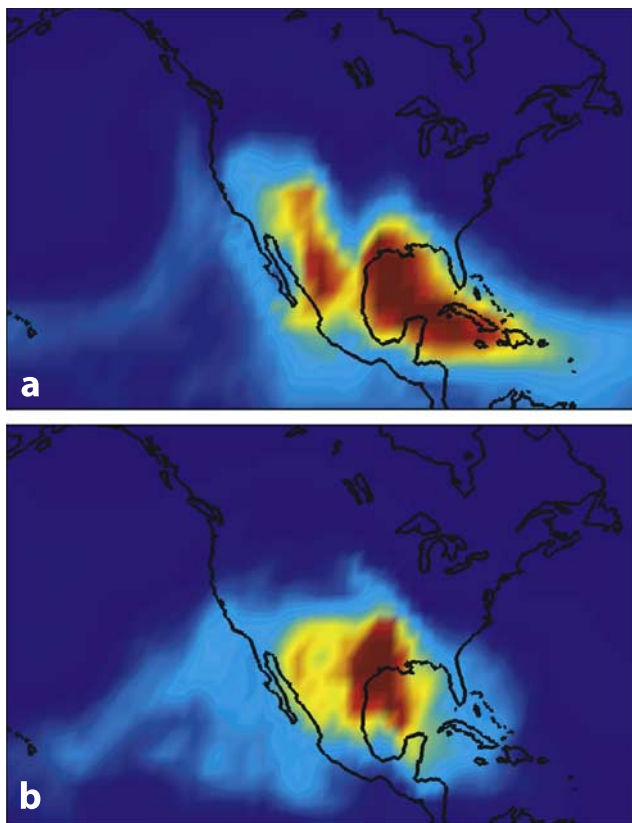
Figure 9. (a) Twenty-day retroplumes run for each 500 m layer between 6 and 12 km above Houston. The residence times of the particles that passed through the 300 m layer adjacent to the Earth's surface were tabulated and averaged over all retroplumes. This image depicts the surface locations with the highest incidence of transport to the 6–12 km region above Houston in arbitrary residence time units. (b) As in Figure 9a but the residence time is tabulated for the atmosphere above 5 km. The arbitrary units in Figure 9a had to be increased by a factor of 100 to put them on the same color scale as Figure 9b. Therefore the quantity of air transported from the regions in Figure 9a is small compared to transport from regions in Figure 9b.

CO at the two sites. While the lower troposphere of the Los Angeles region is heavily polluted, the emissions do not reach the upper troposphere because of a lack of deep convection above coastal southern California. Therefore the CO above LA is representative of CO emissions upwind of North America. Despite Texas being located in the south central United States the upper troposphere above east Texas is no more polluted than the upper tropospheric background air entering the southwestern USA above Los Angeles. In contrast, the eastern sites of Atlanta and Montreal, and the combined sites of New York City/Boston show significantly more CO in the upper troposphere in comparison to Los Angeles. The excess CO is the result of North American anthropogenic CO emissions that are lofted to the upper troposphere across the eastern half of the continent. Above Montreal, and New York City/Boston there was also an influence from CO emissions from the widespread boreal fires in Alaska and western Canada

during the summer of 2004. We also compared the MOZAIC CO profiles above Texas to the 60 MOZAIC CO profiles available at Caracas between 2002 and 2004 (not shown) and found no statistically significant difference between the two locations above 5 km.

[45] Figure 9 shows the average source regions of air in the upper troposphere above Houston as determined by the FLEXPART retroplumes released from the ozone profiles. On average 15% of the upper tropospheric air above Houston passed through the mixed layer during the previous 20 days. Figure 9a shows where the retroplumes from the upper troposphere intercepted the lowest 300 m of the atmosphere. While the retroplumes clearly passed over the high emission regions of Houston and the northern coast of the Gulf of Mexico, most of the influence is from the cleaner regions of the Gulf of Mexico, southwestern USA and northern Mexico. Figure 9b shows the location of the upper tropospheric retroplumes in the atmosphere above the 5 km level. Most of the influence is from the south-central and southwestern USA, northern Mexico and the Gulf of Mexico, with little influence from the eastern or southeastern USA. This transport analysis appears to explain why the MOZAIC aircraft did not detect high levels of pollution above east Texas in the upper troposphere.

3.5. Dominance of Lightning NO_x Above Eastern North America

[46] As shown in Figure 8 and as will be demonstrated below with the FLEXPART simulations the upper troposphere above Houston has a smaller impact from anthropogenic pollution sources than the ozone profile sites along the east coast, even though it has the greatest ozone enhancements. Therefore the in situ ozone production impacting Houston must have a strong contribution from lightning NO_x, a reasonable assumption given that research over the past 30 years has established that lightning is the largest global source of NO_x in the upper troposphere [*Tuck*, 1976; *Chameides et al.*, 1977; *Singh et al.*, 1996; *Huntrieser et al.*, 1998; *Levy et al.*, 1999; *Rakov and Uman*, 2003]. Lightning NO_x emissions are particularly strong above southeastern North America where *Ridley et al.* [2004] described Florida thunderstorms as a faucet of reactive nitrogen to the upper troposphere. Measurements from the NASA DC-8 aircraft support a strong lightning NO_x source in the upper troposphere during ICARTT. Figure 10a shows all of the 10-s average NO_x measurements from the DC-8 above North America between 105 and 64°W during the ICARTT study period. The upper tropospheric mixing ratios are almost as great as the lower tropospheric mixing ratios.

[47] Figure 10b shows the DC-8 NO_x measurements vs. *i*-pentane measurements. Both trace gases are emitted from fossil fuel combustion. Below 2 km the two trace gases are correlated, but above 8 km they are not. Because *i*-pentane has a much longer lifetime than NO_x we expect its mixing ratio to increase with respect to NO_x in the upper troposphere. Instead the opposite is observed with the full range of *i*-pentane mixing ratios associated with NO_x mixing ratios greater than 500 pptv, indicating an additional source of NO_x. One possible source is the lower stratosphere where summertime mixing ratios above eastern North America are typically in the 100–300 pptv range with almost all values below 400 pptv [*Brunner et al.*, 2001]. Because Figure 10b
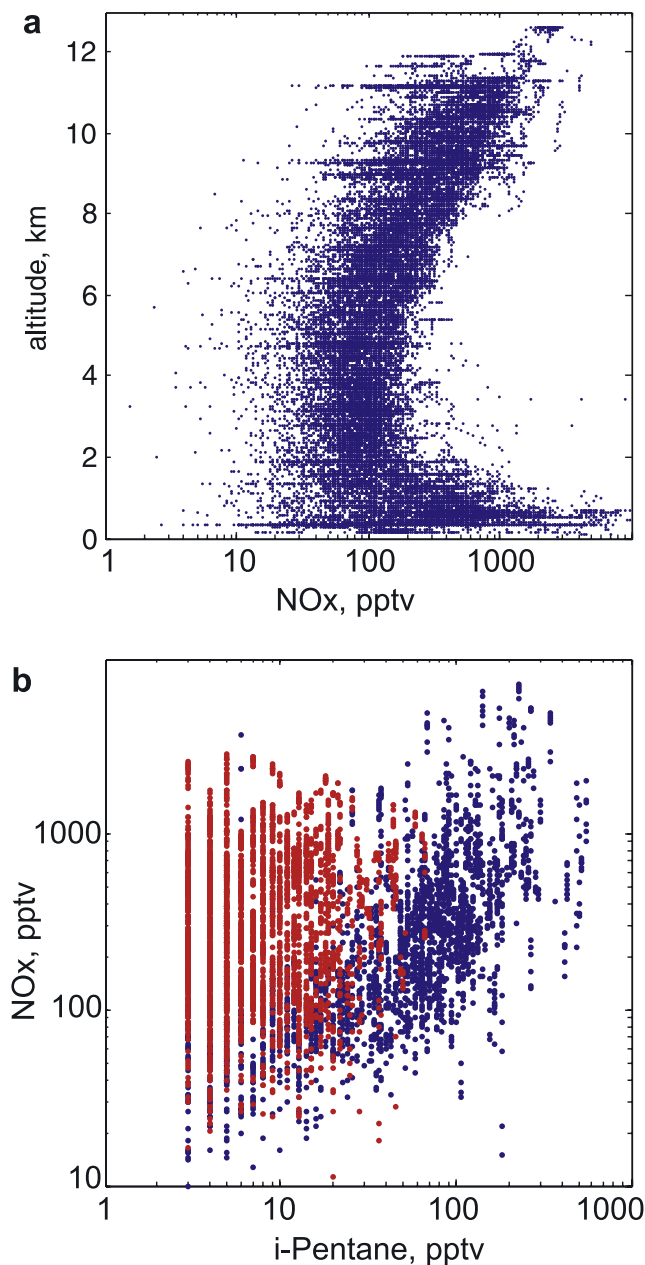
Figure 10. All available 10-s average measurements from the NASA DC-8 from all flights between 1 July and 15 August 2004. (a) Altitude versus NO_x and (b) NO_x versus *i*-pentane below 2 km (blue) and above 8 km (red).

shows many data points with NO_x greater than 400 pptv and low *i*-pentane values we conclude that the most likely source of the NO_x is from lightning.

[48] To quantify the contribution of lightning NO_x to the total amount of NO_x in the upper troposphere of North America we used FLEXPART to simulate the transport of NO_x emissions from biomass burning, biogenic, lightning, aircraft and surface anthropogenic sources. All tracers were run from 1 July through 15 August, plus a 10-day spin-up time. The average column NO_x values for each tracer above 6 km are shown in Figure 11. The plot includes both a 10-day passive NO_x tracer which is useful for seeing where

the NO_x oxidation products and resulting ozone are transported, and a NO_x tracer with a 2-day *e*-folding lifetime which simulates the decay of NO_x in the upper troposphere and shows where the NO_x primarily exists in the upper troposphere. For both the 10-day passive tracer and 2-day lifetime tracer it is clear that lightning NO_x emissions dominate above eastern North America, followed by anthropogenic surface emissions, with aircraft, biogenic and biomass burning emissions making only small contributions. The 2-day lifetime lightning NO_x maximum is located across northern Mexico, the Gulf of Mexico and the westernmost North Atlantic Ocean. Houston has the greatest column lightning NO_x tracer values while Trinidad Head has the lowest. This distribution is largely the result of (1) the dominance of lightning activity across the north coast of the Gulf of Mexico and (2) enhanced lightning across the mountainous regions of northern Mexico and southwestern USA associated with the July-August North American monsoon. *Ridley et al.* [1994] show measurements of high levels of lightning NO_x produced in the upper troposphere within the monsoon flow above New Mexico. Much of the lightning NO_x becomes trapped in the upper troposphere above the Gulf of Mexico as it recirculates in the upper tropospheric anticyclone (Figure 6a) [*Li et al.*, 2005] that is linked to the North American Monsoon. The recirculation is evident in Figure 11 showing the 10-day passive lightning NO_x tracer maximum above the Gulf of Mexico. The recirculation is clearly illustrated in the auxiliary animation of the lightning NO_x tracer. The lightning NO_x tracer is most persistent above the Gulf of Mexico, the south-central United States and Mexico. In contrast the lightning NO_x tracer shows a more episodic influence over the rest of east-central North America due to mesoscale convective complexes racing across the Great Plains and weak cold fronts channeling the tracer up the east coast and out into the North Atlantic Ocean.

[49] As will be shown in the next section the NO_x in the upper troposphere can produce ozone above southern North America for up to 10 days because of the recirculation of the air above the southern USA. Therefore the total 10-day passive NO_x tracer should roughly correlate with ozone above North America if the upper tropospheric ozone enhancement is driven by in situ ozone production. Figure 12 shows median tropospheric residual ozone above 6 km at all 15 ozone monitoring sites vs. the average 10-day total NO_x tracer above 6 km. We see that ozone does increase with the total NO_x tracer, with the data falling along a straight line ($r^2 = 0.74$). Houston is located on the far right, with the three upwind sites on the far left. This straight line correlation is only a qualitative illustration of the relationship between the tropospheric residual ozone and the total NO_x tracer in the upper troposphere, a relationship that is not expected to be strictly linear because of the fact that ozone production efficiency varies with NO_x, CO, CH_4, nonmethane hydrocarbons and water vapor mixing ratios as well as sunlight.

[50] If we sum up all of the 2-day lifetime NO_x tracer above the east-central region of North America that encompasses the 12 eastern sites we find that lightning NO_x accounts for 80% of the total (84% above Houston only). However, in this comparison the quantity of NO_x tracer from surface emissions is greatly overestimated because we
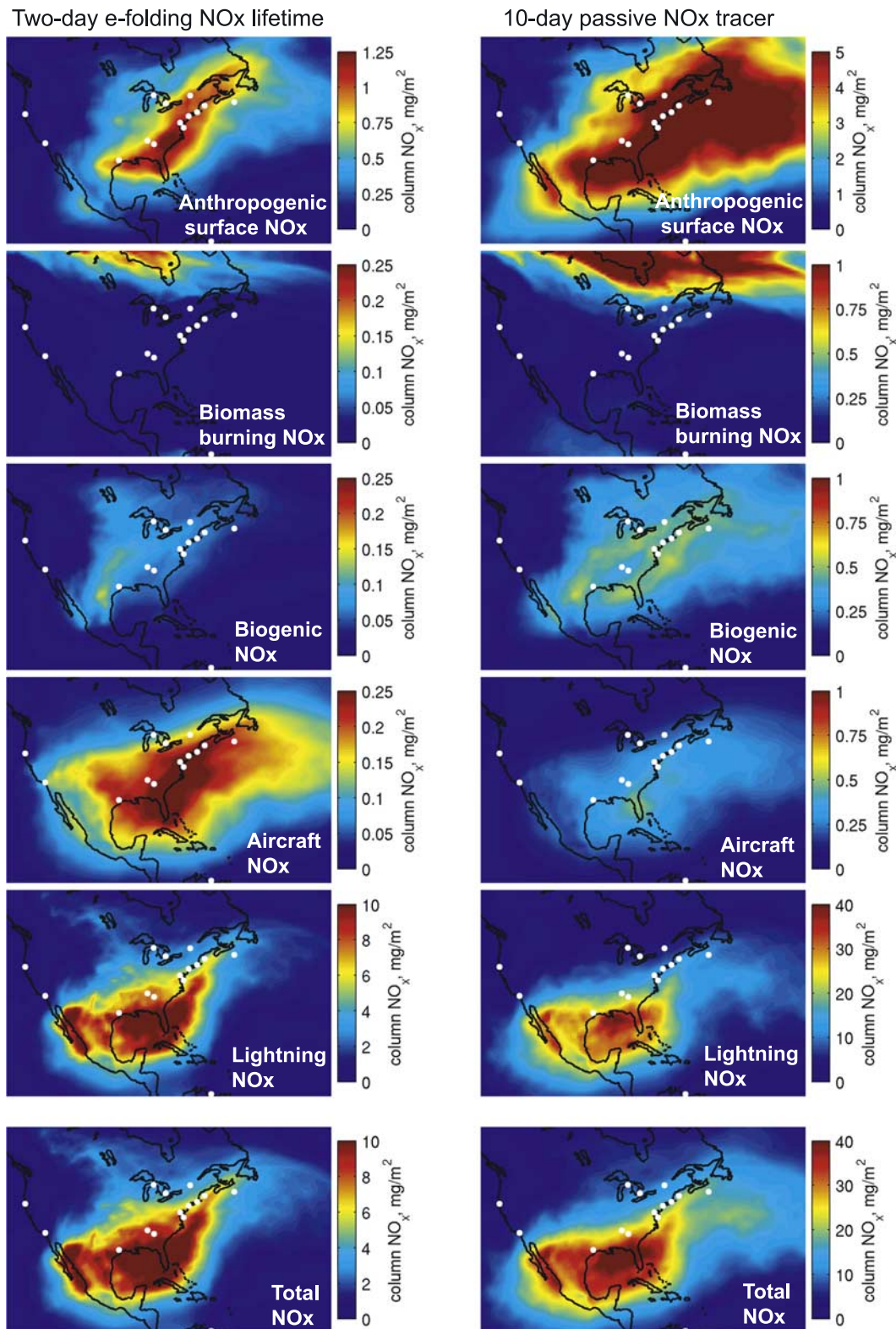
Two-day e-folding NOx lifetime   **10-day passive NOx tracer**

Figure 11. Column NO_x tracers above 6 km averaged over the 1 July to 15 August 2004 time period. NO_x emissions are from surface anthropogenic sources, biomass burning, biogenic soil emissions, aircraft and lightning. The bottom row shows the sum of the five NO_x tracers. (left) Location of the NO_x tracers in the upper troposphere that are allowed to decay with a 2-day *e*-folding lifetime and (right) average locations for passive 10-day NO_x tracers. Note that the color bars on the right are greater than those on the left by a factor of four and that the lightning NO_x color bars are greater than the anthropogenic surface NO_x color bars by a factor of 8 and greater than the biomass burning, biogenic and aircraft NO_x tracers by a factor of 40.
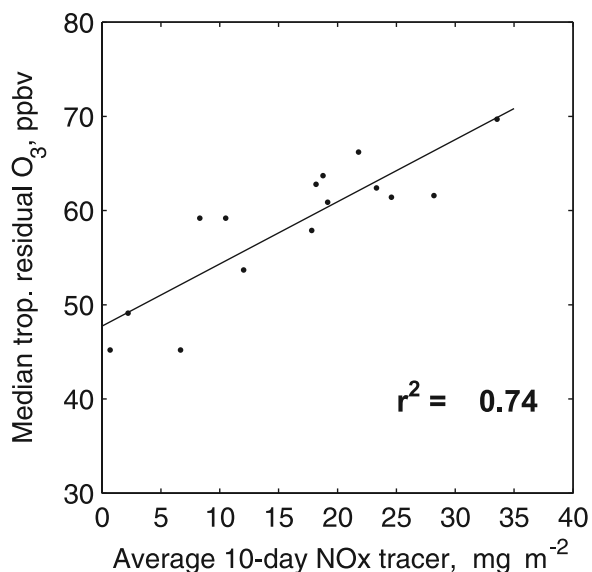
Figure 12. Median tropospheric residual ozone above 6 km (as taken from Figure 4c) versus the average 10-day total NO_x tracer above 6 km (as taken from Figure 11).

have assumed a 2-day NO_x lifetime which is appropriate for the upper troposphere but not for NO_x emitted into the continental boundary layer where the NO_x lifetime is much shorter. *Li et al.* [2004] estimate that at least 80% of surface NO_x emissions never make it out of the continental boundary layer as they are oxidized in the CBL and removed via wet and dry deposition. If we apply this 80% reduction to the surface anthropogenic and biogenic NO_x emissions (but not to the biomass burning emissions as we assume all of the NO_x is rapidly lofted from the boundary layer because of the heat from the fires) we estimate that lightning NO_x is 95% (96%) of the total NO_x above east-central North America (Houston). The lightning NO_x emission rate that we selected for this study is 6.4 kg N flash^{-1}. This value is toward the higher end of widely varying estimates, which can be as low as 1.3 kg N flash^{-1} [*Beirle et al.*, 2006]. Even if we reduce our lightning NO_x emissions by a factor of 5 we find that lightning NO_x still accounts for 78% (83%) of the total above east-central North America (Houston). In a separate GEOS-CHEM model study of the North American reactive nitrogen budget during the ICARTT study period R. C. Hudman et al. (Surface and lightning sources of nitrogen oxides in the United States: Magnitudes, chemical evolution, and outflow, submitted to *Journal of Geophysical Research*, 2006) also conclude that lightning is the primary source of NO_x in the upper troposphere above midlatitude North America.

4. Discussion

[51] In section 3.3 we were conservative and estimated that at least 14 ppbv of the 16 ppbv tropospheric residual ozone enhancement above eastern North America, or 88%, must be due to in situ ozone production in the free troposphere. In section 3.5 we estimated that at least 78% of the NO_x in the upper troposphere above eastern North America must be due to lightning emissions. Therefore, assuming NO_x from all sources produces ozone with the same efficiency, at least 69% (and up to 84%) of the total ozone enhancement above eastern North America is due to in situ production from lightning NO_x. However, can these ozone enhancements really be produced from the estimated NO_x in the upper troposphere, especially above Houston where the ozone enhancement is 24 ppb and the air is not heavily polluted? To answer this question we conducted a box modeling study of ozone production above Houston from lightning NO_x emissions.

[52] We began by retrieving the FLEXPART lightning NO_x tracer values along the NASA DC-8 flight tracks over the continental USA during ICARTT and applying an *e*-folding lifetime to make the modeled values match the median NO_x profile measured by the DC-8. Figure 13 shows the results when lifetimes of 1, 2 and 4 days are used. The 2-day lifetime produces the best fit between the modeled and measured median profiles above 6 km, although the 90th percentile of the modeled lightning NO_x is about a factor of 4 too high. The overestimate at the high end could be due to the DC-8 not intercepting the most concentrated plumes of lightning NO_x. While the DC-8 NO_x measurements reached as high as 5 ppbv, other studies have reported NO measurements as high as 9.5, 19 and 25 ppbv in thunderstorm anvils above Florida [*Ridley et al.*, 2004], Colorado [*Stith et al.*, 1999] and Germany [*Huntrieser et al.*, 2002], respectively. This 2-day lifetime agrees with box model analyses of upper tropospheric NO_x lifetime based on the NASA DC-8 trace gas measurements during ICARTT [*Olson et al.*, 2005]; it also agrees with the NO_x lifetime calculated by Bertram et al. (manuscript in preparation, 2006) at 10 km, although their NO_x lifetime at 12 km is longer and fresh NO_x injections require 6 days to achieve steady state mixing ratios. To account for the possibility that our lightning NO_x emission rate of 6.4 kg N flash^{-1} is too high we conducted a second box model study using an emission rate of 3.2 kg N flash^{-1}. This lower emission rate requires a NO_x lifetime in the upper troposphere of 5 days to force the NO_x tracer to match the DC-8 NO_x measurements. This 5-day lifetime falls in the range of values determined by *Jaeglé et al.* [1998] for April-May conditions above the USA, and may be more appropriate given that both the NASA Langley photochemical box model and the model used by Bertram et al. (manuscript in preparation, 2006) produced greater OH mixing ratios than those observed by the DC-8, which means the actual NO_x lifetime in the upper troposphere could be longer than 2 days.

[53] Next, for the times when we had ozone measurements from the IONS and MOZAIC profiles in the upper troposphere, we calculated the net ozone production upwind of Houston over a 10 day period. This was based on the upwind distribution of FLEXPART NO_x between 9 and 12 km with a 2-day lifetime and median upper tropospheric trace gas mixing ratios for relatively clean conditions during INTEX. These clean conditions were based on DC-8 observations in the upper troposphere when CO mixing ratios were less than 100 ppbv, and were chosen to match the MOZAIC CO measurements above east Texas. Calculations were performed using the NASA Langley photochemical box model to provide diurnal-average estimates of net ozone production over each of the 10 days. The most recent
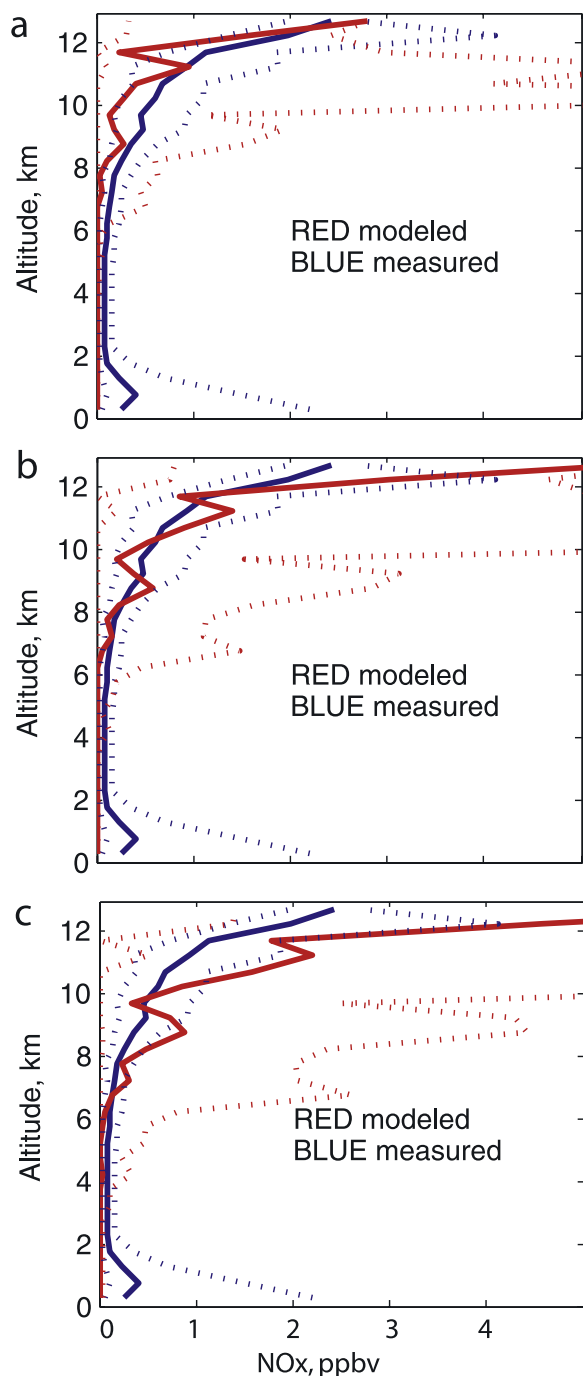
Figure 13. Distributions of measured NO_x (blue) from the DC8 above eastern North America during 1 July to 15 August 2004 and the corresponding FLEXPART lightning NO_x tracer values (red). Shown are the median values (solid lines) and the 10th and 90th percentiles (dashed lines) with modeled NO_x lifetimes of (a) 1 day, (b) 2 days, and (c) 4 days.

description of the model is given by *Olson et al.* [2006]. On the basis of these calculations and using a lightning NO_x emission rate of 6.4 kg N flash^{-1}, a net increase in ozone of 29 ppbv could be achieved over the 10 days, accounting for an upper tropospheric ozone lifetime of approximately 90 days. When we removed the relatively small concentrations of reactive nonmethane hydrocarbons the net ozone production was 27 ppbv, indicating that large quantities of ozone can be produced even in the absence of fresh anthropogenic emissions. Under these conditions the ozone production is primarily the result of reactions between relatively high lightning NO_x mixing ratios and background mixing ratios of CO and CH_4.

[54] When we applied a lightning NO_x emission rate of 3.2 kg N flash^{-1}, the model still produced a net ozone increase of 27 ppbv. This result should not be surprising since the largest changes in the NO_x distribution occurred for the very high NO_x levels (exceeding several ppbv). At ppbv levels, NO_x becomes the dominant sink for the peroxy radicals that facilitate ozone production, thus further increases in NO_x lead to much less efficient production. Instead, most of the ozone increase is associated with the more efficient production in air parcels containing several hundred pptv of NO_x which are abundant in both NO_x distributions. When considering the NO_x distribution observed by the DC-8 which lacked the extremely high values (see Figure 13b), the average calculated ozone net production rate is approximately 4 ppbv/day. This production rate could result in an additional 24 ppbv of ozone in about 6–7 days if the NO_x distribution can be sustained.

[55] From this analysis we conclude that the upper troposphere above the southern USA contains sufficient lightning NO_x to produce a median ozone enhancement of 24 ppbv through oxidation reactions of relatively enhanced NO_x and background mixing ratios of CH_4 and CO alone. While lightning dominates the upper tropospheric NO_x budget above eastern North America the ozone production from lightning NO_x should not be treated as a purely natural process because emissions of nonmethane hydrocarbons and especially CO and CH_4 are required to produce the ozone, with anthropogenic sources accounting for roughly 60% of CH_4 emissions and 50% of CO emissions [*Fiore et al.*, 2002].

[56] We also examined the potential ozone production in the upper troposphere above Texas when lightning NO_x emissions were switched off. Combined emissions from surface anthropogenic, biogenic, biomass burning and aircraft emissions resulted in a 6 ppbv net ozone production over 10 days for a 2-day NO_x lifetime and 11 ppbv for a 5-day lifetime. While these NO_x mixing ratios were 10–20 times less than the lightning NO_x mixing ratios they produced disproportionately more ozone because of the greater ozone production efficiency at lower NO_x mixing ratios. Regardless of NO_x lifetime these emissions account for less than half of the ozone enhancement above Houston. In reality the nonlightning NO_x does not produce ozone independently from the lightning NO_x. Ozone production from lightning NO_x and nonlightning NO_x above Houston cannot simply be added together because of the nonlinearity of ozone production and the reduced ozone production efficiency at higher NO_x mixing ratios. The nonlightning NO_x is dispersed into the upper troposphere that is already dominated by lightning NO_x emissions. Because the NO_x molecules from the different sources collectively reduce the ozone production efficiency in this environment, lightning NO_x and nonlightning NO_x should be treated as equally productive on a per molecule basis

and we come back to our broad estimate of lightning NO_x being responsible for 69–84% of the ozone enhancement above eastern North America (as described at the beginning of section 4).

[57]　*Moxim and Levy* [2000] conducted a chemical transport model study of ozone above the tropical South Atlantic Ocean. They found that the upper tropospheric ozone maximum above this region was dominated by ozone production from lightning NO_x in conjunction with CO/CH_4 chemistry. They suggested an ozone maximum would have existed in this region in preindustrial times. Along these lines we suggest that an upper tropospheric ozone enhancement would have existed above eastern North America during preindustrial times because of ozone production from lightning NO_x and background mixing ratios of CO and CH_4. While such an analysis is beyond the scope of this paper we speculate that the ozone enhancement would have been smaller than the present-day enhancement because of the greatly reduced anthropogenic emissions of NO_x, CO and CH_4.

5. Conclusions

[58]　This study assembled the most comprehensive set of ozone measurements ever collected in the free troposphere above midlatitude North America during a single season. By focusing on measurements taken only in the troposphere and by calculating and subtracting the influence from aged stratospheric intrusions (up to 20 days old) we produced a data set of tropospheric residual ozone values across the study region. On average the upper troposphere above midlatitude eastern North America contained 15 ppbv more tropospheric residual ozone than the more polluted layer between the surface and 2 km above sea level (Figure 4c). Furthermore the upper troposphere above midlatitude eastern North America contained 16 ppbv more tropospheric residual ozone than the upper troposphere above 3 upwind sites, with the greatest enhancement above Houston at 24 ppbv (Figure 7d). Our detailed simulation of lightning NO_x emissions tied to the exact times and locations of actual cloud-to-ground lightning flashes across North America shows that lightning is the dominant source of NO_x in the upper troposphere. Overall, we estimate that 69–84% (11–13 ppbv) of the 16 ppbv ozone enhancement above eastern North America is due to in situ ozone production from lightning NO_x with the remainder due to transport of ozone from the surface or in situ ozone production from other sources of NO_x.

[59]　This study contains several sources of uncertainty, greatest of which are the lightning NO_x emission rate and the lifetime of NO_x in the upper troposphere, and we have been careful to take the variability of these values into account. We have provided some broad estimates of the lightning NO_x contribution to the widespread upper tropospheric ozone enhancement across eastern North America, and additional chemical transport model studies and measurements are required to refine the quantification of the contribution of lightning NO_x to the upper tropospheric ozone enhancement for the individual measurement stations. However, some confirmation of our results is provided by a recent study that showed great foresight into the existence of the upper tropospheric ozone maximum above

Texas. *Li et al.* [2005] used a global-scale chemical transport model to simulate ozone production above North America for the summer of 2000. They predicted that an ozone maximum would be present in the upper troposphere above the south-central USA as a result of convective lofting of surface ozone, and in situ production by anthropogenic NO_x, lightning NO_x, and formaldehyde produced from surface isoprene emissions. Long residence times in the upper troposphere due to the recirculation in the semipermanent summertime anyticyclone would allow for ozone production over several days. Ozone measurements were limited for the study period and only 6 profiles above Huntsville, Alabama were available to validate the simulation. Interestingly, the authors found that they had to increase the model-generated lightning NO_x by a factor of 4 above the standard simulation to make the model match the ozonesonde measurements, indicating the importance of lightning NO_x in this region. Our tropospheric residual ozone distribution across the North American upper troposphere confirms the modeling results of *Li et al.* [2005], with much of the ozone distribution related to the recirculation in the upper tropospheric anticyclone centered over southern North America. However, we place greater emphasis on the role of lightning NO_x in producing the ozone enhancement.

[60]　While this study has revealed an upper tropospheric ozone maximum centered above Houston we only know that its production begins somewhere east of the west coast and somewhere north of Caracas, Venezuela. Additional ozone profiles are required in western North America and south of the USA to identify where the ozone maximum begins. Another key site on the west coast would be the southern coast of British Columbia to determine if Trinidad Head and Table Mountain are truly representative of air flowing into western North America. Profiles in central Mexico, and at the New Mexico/Mexico border would indicate the amount of ozone flowing into the southern USA with the North American monsoon, while additional profiles in Colorado and Saskatchewan would reveal the northerly extent of this influence. Finally, profiles are needed from the eastern edge of the Caribbean Sea. This location would measure the background ozone that flows from the tropical North Atlantic Ocean into the Gulf of Mexico and on to the southern USA via the North American monsoon flow, while being positioned upwind of the major North American lightning region.

References

Beirle, S., et al. (2006), Estimating the NO_x produced by lightning from GOME and NLDN data: A case study in the Gulf of Mexico, *Atmos. Chem. Phys.*, *6*, 1075–1089.

Boccippio, D. J., K. L. Cummins, H. J. Christian, and S. J. Goodman (2001), Combined satellite- and surface-based estimation of the intra-cloud-cloud-to-ground lightning ratio over the continental United States, *Mon. Weather Rev.*, *129*, 108–122.

Brunner, D., J. Staehelin, D. Jeker, and H. Wernli (2001), Nitrogen oxides and ozone in the tropopause region of the Northern Hemisphere: Measurements from commercial aircraft in 1995/1996 and 1997, *J. Geophys. Res.*, *106*, 27,673–27,699.

Cleary, P. A., P. J. Wooldridge, and R. C. Cohen (2002), Laser-induced fluorescence detection of atmospheric NO_2 with a commercial diode laser and a supersonic expansion, *Appl. Opt.*, *41*, 6950–6956.

Chameides, W. L., D. H. Stedman, R. R. Dickerson, D. W. Rusch, and R. J. Cicerone (1977), NO_x production in lightning, *J. Atmos. Sci.*, *34*, 143–149.

Christian, H. J., et al. (2003), Global frequency and distribution of lightning as observed from space by the Optical Transient Detector, *J. Geophys. Res.*, *108*(D1), 4005, doi:10.1029/2002JD002347.

Colman, J. J., A. L. Swanson, S. Meinardi, B. C. Sive, D. R. Blake, and F. S. Rowland (2001), Description of the analysis of a wide range of volatile organic compounds in whole air samples collected during PEM-Tropics A and B, *Anal. Chem.*, *73*(15), 3723–3731, doi:10.1021/ac010027g.

Cooper, O. R., J. L. Moody, D. D. Parrish, M. Trainer, T. B. Ryerson, J. S. Holloway, G. Hübler, F. C. Fehsenfeld, and M. J. Evans (2002), Trace gas composition of midlatitude cyclones over the western North Atlantic Ocean: A conceptual model, *J. Geophys. Res.*, *107*(D7), 4056, doi:10.1029/2001JD000901.

Cooper, O. R., et al. (2005a), A springtime comparison of tropospheric ozone and transport pathways on the east and west coasts of the United States, *J. Geophys. Res.*, *110*, D05S90, doi:10.1029/2004JD005183.

Cooper, O. R., et al. (2005b), Direct transport of midlatitude stratospheric ozone into the lower troposphere and marine boundary layer of the tropical Pacific Ocean, *J. Geophys. Res.*, *110*, D23310, doi:10.1029/2005JD005783.

DeCaria, A. J., K. E. Pickering, G. L. Stenchikov, and L. E. Ott (2005), Lightning-generated NO_x and its impact on tropospheric ozone production: A three-dimensional modeling study of a Stratosphere-Troposphere Experiment: Radiation, Aerosols and Ozone (STERAO-A) thunderstorm, *J. Geophys. Res.*, *110*, D14303, doi:10.1029/2004JD005556.

Emanuel, K. A., and M. Živković-Rothman (1999), Development and evaluation of a convection scheme for use in climate models, *J. Atmos. Sci.*, *56*, 1766–1782.

Fiore, A. M., D. J. Jacob, and J. A. Logan (1998), Long-term trends in ground level ozone over the contiguous United States, 1980–1995, *J. Geophys. Res.*, *103*, 1471–1480.

Fiore, A. M., D. J. Jacob, B. D. Field, D. G. Streets, S. D. Fernandes, and C. Jang (2002), Linking ozone pollution and climate change: The case for controlling methane, *Geophys. Res. Lett.*, *29*(19), 1919, doi:10.1029/2002GL015601.

Fishman, J., and A. E. Balok (1999), Calculation of daily tropospheric ozone residuals using TOMS and empirically improved SBUV measurements: Application to an ozone pollution episode over the eastern United States, *J. Geophys. Res.*, *104*, 30,319–30,340.

Fishman, J., C. E. Watson, J. C. Larsen, and J. A. Logan (1990), Distribution of troposphere ozone determined from satellite data, *J. Geophys. Res.*, *95*, 3599–3617.

Forster, C., A. Stohl, P. James, and V. Thouret (2003), The residence times of aircraft emissions in the stratosphere using a mean emission inventory and emissions from actual flight tracks, *J. Geophys. Res.*, *108*(D12), 8524, doi:10.1029/2002JD002515.

Forster, C., A. Stohl, and P. Seibert (2006), Parameterization of convective transport in a Lagrangian particle dispersion model and its evaluation, *J. Appl. Meteorol. Clim.*, in press.

Frost, G. J., et al. (2006), Effects of changing power plant NO_x emissions on ozone in the eastern United States: Proof of concept, *J. Geophys. Res.*, *111*, D12306, doi:10.1029/2005JD006354.

Grogan, M. J. (2004), Report on the 2002–2003 US NLDN system-wide upgrade, Vaisala Thunderstorm, Tuscon, Ariz. (Available at http://www.vaisala.com/businessareas/measurementsystems/thunderstorm/knowledgecenter/aboutnldn)

Huntrieser, H., H. Schlager, C. Feigl, and H. Höller (1998), Transport and production of NO_x in electrified thunderstorms: Survey of previous studies and new observations at midlatitudes, *J. Geophys. Res.*, *103*(D21), 28,247–28,264.

Huntrieser, H., et al. (2002), Airborne measurements of NO_x, tracer species, and small particles during the European Lightning Nitrogen Oxides Experiment, *J. Geophys. Res.*, *107*(D11), 4113, doi:10.1029/2000JD000209.

Intergovernmental Panel on Climate Change (2001), *Climate Change 2001: The Scientific Basis—Contribution of Working Group I to the Third Assessment Report of the Intergovernmental Panel on Climate Change*, edited by J. T. Houghton et al., 881 pp., Cambridge Univ. Press, New York.

Jaeglé, L., D. J. Jacob, Y. Wang, A. J. Weinheimer, B. A. Ridley, T. L. Campos, G. W. Sachse, and D. E. Hagen (1998), Sources and chemistry of NOx in the upper troposphere over the United States, *Geophys. Res. Lett.*, *25*, 1705–1708.

Levy, H., II, W. J. Moxim, A. A. Klonecki, and P. S. Kasibhatla (1999), Simulated tropospheric NO_x: Its evaluation, global distribution and individual source contributions, *J. Geophys. Res.*, *104*, 26,279–26,306.

Li, Q., et al. (2002), Transatlantic transport of pollution and its effects on surface ozone in Europe and North America, *J. Geophys. Res.*, *107*(D13), 4166, doi:10.1029/2001JD001422.

Li, Q., D. J. Jacob, J. W. Munger, R. M. Yantosca, and D. D. Parrish (2004), Export of NOy from the North American boundary layer: Reconciling aircraft observations and global model budgets, *J. Geophys. Res.*, *109*, D02313, doi:10.1029/2003JD004086.

Li, Q., D. J. Jacob, R. Park, Y. Wang, C. L. Heald, R. Hudman, R. M. Yantosca, R. V. Martin, and M. Evans (2005), North American pollution outflow and the trapping of convectively lifted pollution by upper-level anticyclone, *J. Geophys. Res.*, *110*, D10301, doi:10.1029/2004JD005039.

McDermid, I. S., G. Beyerle, D. A. Haner, and T. Leblanc (2002), Redesign and improved performance of the tropospheric ozone lidar at the Jet Propulsion Laboratory Table Mountain Facility, *Appl. Opt.*, *41*, 7550–7555.

Merrill, J. T., and J. L. Moody (1996), Synoptic meteorology and transport during the North Atlantic Regional Experiment (NARE) intensive: Overview, *J. Geophys. Res.*, *101*, 28,903–28,921.

Moody, J. L., J. C. Davenport, J. T. Merrill, S. J. Oltmans, D. D. Parrish, J. S. Holloway, H. Levy, G. L. Forbes, M. Trainer, and M. Buhr (1996), Meteorological mechanisms for transporting O_3 over the western North Atlantic ocean: A case study for August 24–29, 1993, *J. Geophys. Res.*, *101*, 29,213–29,227.

Mortlock, A. M., and R. Van Alstyne (1998), Military, charter, unreported domestic traffic and general aviation: 1976, 1984, 1992, and 2015 emission scenarios, *NASA CR-1998-207639*. (Available at http://ntrs.nasa.gov/archive/nasa/casi.ntrs.nasa.gov/19980047346_1998120131.pdf)

Moxim, W. J., and H. Levy II (2000), A model analysis of he tropical South Atlantic Ocean tropospheric ozone maximum: The interaction of transport and chemistry, *J. Geophys. Res.*, *105*, 17,393–17,415.

Nedelec, P., J.-P. Cammas, V. Thouret, G. Athier, J.-M. Cousin, C. Legrand, C. Abonnel, F. Lecoeur, G. Cayez, and C. Marizy (2003), An improved infrared carbon monoxide analyser for routine measurements aboard commercial Airbus aircraft: technical validation and first scientific results of the MOZAIC III programme, *Atmos. Chem. Phys.*, *3*, 1551–1564.

Newchurch, M. J., M. A. Ayoub, S. Oltmans, B. Johnson, and F. J. Schmidlin (2003), Vertical distribution of ozone at four sites in the United States, *J. Geophys. Res.*, *108*(D1), 4031, doi:10.1029/2002JD002059.

Olivier, J. G. J., and J. J. M. Berdowski (2001), Global emissions sources and sinks, in *The Climate System*, edited by J. Berdowski, R. Guicherit, and B. J. Heij, pp. 33–78, A. A. Balkema, Brookfield, Vt.

Olson, J. R., et al. (2005), An examination of photochemical theory based on INTEX-NA observations, *Eos Trans. AGU*, *86*(52), Fall Meet. Suppl., Abstract A51C-0063.

Olson, J. R., J. H. Crawford, G. Chen, W. H. Brune, I. C. Faloona, D. Tan, H. Harder, and M. Martinez (2006), A reevaluation of airborne HOx observations from NASA field campaigns, *J. Geophys. Res.*, *111*, D10301, doi:10.1029/2005JD006617.

Orville, R. E., G. R. Huffines, W. R. Burrows, R. L. Holle, and K. L. Cummins (2002), The North American Lightning Detection Network (NALDN)—First results: 1998–2000, *Mon. Weather Rev.*, *130*, 2098–2109.

Pickering, K. E., Y. Wang, W.-K. Tao, C. Price, and J.-F. Müller (1998), Vertical distributions of lightning NO_x for use in regional and global chemical transport models, *J. Geophys. Res.*, *103*(D23), 31,203–31,216.

Pierce, T., C. Geron, L. Bender, R. Dennis, G. Tonneson, and A. Guenther (1998), Influence of increased isoprene emissions on regional ozone modeling, *J. Geophys. Res.*, *103*, 25,611–25,629.

Rakov, V. A., and M. A. Uman (2003), *Lightning: Physics and Effects*, 687 pp., Cambridge Univ. Press, New York.

Ridley, B. A., J. G. Walega, J. E. Dye, and F. E. Grahek (1994), Distributions of NO, NO_x, NO_y and O_3 to 12 km altitude during the summer monsoon season over New Mexico, *J. Geophys. Res.*, *99*, 25,519–25,534.

Ridley, B., et al. (2004), Florida thunderstorms: A faucet of reactive nitrogen to the upper troposphere, *J. Geophys. Res.*, *109*, D17305, doi:10.1029/2004JD004769.

Ridley, B. A., K. E. Pickering, and J. E. Dye (2005), Comments on the parameterization of lightning-produced NO in global chemistry-transport models, *Atmos. Environ.*, *39*, 6184–6187.

Singh, H. B., et al. (1996), Reactive nitrogen and ozone over the western Pacific: Distribution, partitioning, and sources, *J. Geophys. Res.*, *101*, 1793–1808.

Stith, J., J. Dye, B. Ridley, P. Laroche, E. Defer, K. Baumann, G. Hübler, R. Zerr, and M. Venticinque (1999), NO signatures from lightning flashes, *J. Geophys. Res.*, *104*, 16,081–16,090.

Stohl, A., M. Hittenberger, and G. Wotawa (1998), Validation of the Lagrangian particle dispersion model FLEXPART against large scale tracer experiment data, *Atmos. Environ.*, *32*, 4245–4264.

Stohl, A., C. Forster, S. Eckhardt, N. Spichtinger, H. Huntrieser, J. Heland, H. Schlager, H. Aufmhoff, F. Arnold, and O. Cooper (2003), A backward modeling study of intercontinental pollution transport using aircraft measurements, *J. Geophys. Res.*, *108*(D12), 4370, doi:10.1029/2002JD002862.

Stohl, A., C. Forster, A. Frank, P. Seibert, and G. Wotowa (2005), Technical note: The Lagrangian particle dispersion model FLEXPART version 6.2, *Atmos. Chem. Phys.*, *5*, 2461–2474.

Sutkus, D. J., Jr., S. L. Baughcum, and D. P. DuBois (2001), Scheduled civil aircraft emission inventories for 1999: Database development and analysis, *NASA/CR-2001-211216*.

Tarasick, D. W., V. E. Fioletov, D. I. Wardle, J. B. Kerr, and J. Davies (2005), Changes in the vertical distribution of ozone over Canada from ozonesondes: 1980–2001, *J. Geophys. Res.*, *110*, D02304, doi:10.1029/2004JD004643.

Thornton, J. A., P. J. Wooldridge, and R. C. Cohen (2000), Atmospheric NO_2: In situ laser-induced fluorescence detection at parts per trillion mixing ratios, *Anal. Chem.*, *72*, 528–539.

Thouret, V., A. Marenco, J. A. Logan, P. Nédélec, and C. Grouhel (1998), Comparisons of ozone measurements from the MOZAIC airborne program and the ozone sounding network at eight stations, *J. Geophys. Res.*, *103*, 25,695–25,720.

Tuck, A. F. (1976), Production of nitrogen oxides by lightning discharges, *Q. J. R. Meteorol. Soc.*, *102*, 749–755.

Yienger, J. J., and H. Levy II (1995), Empirical model of global soil-biogenic NO_x emissions, *J. Geophys. Res.*, *100*, 11,447–11,464.

Zipser, E. J., D. J. Cecil, C. Liu, S. W. Nesbitt, and D. P. Yorty (2006), Where are the most intense thunderstorms on Earth?, *Bull. Am. Meteorol. Soc.*, *87*, 1057–1071.

S. L. Baughcum, Boeing Company, Seattle, WA 98124, USA.

T. H. Bertram, R. C. Cohen, A. Perring, and P. Wooldridge, Department of Chemistry, University of California, Berkeley, CA 94720, USA.

C. C. Brown, G. Chen, and J. H. Crawford, NASA Langley Research Center, Hampton, VA 23681-2199, USA.

W. H. Brune, X. Ren, and A. M. Thompson, Department of Meteorology, Pennsylvania State University, University Park, PA 16802, USA.

O. R. Cooper, F. C. Fehsenfeld, B. J. Johnson, S. A. McKeen, J. F. Meagher, S. J. Oltmans, and M. Trainer, NOAA Earth System Research Laboratory, Chemical Sciences Division, Theoretical Aeronomy Branch, CSD04, 325 Broadway, Boulder, CO 80305, USA. (owen.r.cooper@noaa.gov)

G. Forbes, Meteorological Service of Canada, Sable Island, NS, Canada B3J 2L4.

T. Leblanc and I. S. McDermid, Table Mountain Facility, Jet Propulsion Laboratory, California Institute of Technology, Wrightwood, CA 92397, USA.

J. Merrill, Graduate School of Oceanography, University of Rhode Island, Narragansett, RI 02882, USA.

J. L. Moody, Department of Environmental Sciences, University of Virginia, Charlottesville, VA 22093, USA.

G. Morris, Department of Physics and Astronomy, Valparaiso University, Valparaiso, IN 46383, USA.

P. Nédélec, Laboratoire d'Aerologie, Centre National de la Recherche Scientifique, Observatoire Midi-Pyrenees, F-31400 Toulouse, France.

M. J. Newchurch, Atmospheric Science Department, University of Alabama, Huntsville, AL 35805, USA.

K. E. Pickering, Laboratory for Atmospheres, NASA Goddard Space Flight Center, Greenbelt, MD 20771, USA.

F. J. Schmidlin, Wallops Flight Facility, NASA Goddard Space Flight Center, Wallops Island, VA 23337, USA.

N. Spichtinger, Department of Ecology, Technical University of Munich, D-80333 Freising-Weihenstephan, Germany.

A. Stohl, Norwegian Institute for Air Research, N-2027 Kjeller, Norway.

D. Tarasick, Experimental Studies Research Division, Meteorological Service of Canada, Environment Canada, Downsview, ON, Canada M3H 5T4.

S. Turquety, Service d'Aéronomie, Institut Pierre-Simon Laplace, Université Pierre et Marie Curie, F-75005 Paris, France.

J. C. Witte, Science Systems and Applications, Inc., NASA Goddard Space Flight Center, Greenbelt, MD 20770, USA.